

UNPUBLISHED PRELIMINARY DATA

STRESS ANALYSIS OF CRACKS

by

Paul C. Paris

George C. Sih

REPORTS CONTROL No. _____

Department of Mechanics

Lehigh University

Bethlehem, Pennsylvania

June, 1964

This work was supported by a grant from The National Aeronautics and Space Administration, Nsg 410, and presents results in part from earlier grants by The Boeing Company and The National Science Foundation to the Lehigh Institute of Research.

ALL INFORMATION CONTAINED
HEREIN IS UNCLASSIFIED

DATE 08-11-2001 BY SP-10/STP

This is an advance copy of a paper to be presented at the Sixty-Seventh Annual Meeting of the American Society for Testing and Materials (1916 Race Street, Philadelphia 3, Pa.) to be held in Chicago, Ill., June 21-26. This advance copy is primarily to stimulate discussion. Discussion is invited and may be transmitted to the Executive Secretary. The paper is subject to modification and is not to be published as a whole or in part pending its release by the Society through the Executive Secretary.

Table of Contents

Abstract	- 1 -
Introduction	1
Crack Tip Stress Fields for Isotropic Elastic Bodies	2
Elementary Dimensional Considerations for Determination of Stress Intensity Factors	7
Stress-Intensity-Factors from Westergaard Stress Functions	10
Stress-Intensity-Factors from General Complex Stress Functions	15
Stress-Intensity-Factors for Some Three-Dimensional Cases	19
Edge Cracks in Semi-Infinite Bodies	22
Two-Dimensional Problems of Plate Strips with Transverse Cracks	24
Reinforced Plane Sheets	31
Thermal Stresses	32
Stress-Intensity-Factors for the Bending of Plates and Shells	34
Couple Stress Problems with Cracks	40
Estimation of Stress Intensity Factors for some Cases of Practical Interest	41

Stress Fields and Intensity Factors for Homogeneous Anisotropic Media	50
Cracks in Linear Visco-Elastic Media	61
Some Special Cases of Non-Homogeneous Media with Cracks	63
Inertia Effects on the Stress Field of a Moving Crack	65
Energy Rate Analysis of Crack Extension	67
The Equivalence of Energy Rate and Stress-Intensity-Factor Approaches	69
Other Equivalent Methods of Stress Analysis of Cracks and Notches	73
Limitations of Crack Tip Stress Field Analyses	75
Acknowledgement	80
References	81
Table of Notation	90
Figures	94
Appendix I - The Westergaard Method of Stress Analysis of Cracks	A-1
Appendix II - A Handbook of Basic Solutions for Stress-Intensity-Factors and other Formulas	B-1

STRESS ANALYSIS OF CRACKS

by

P. Paris & G. Sih

Abstract:

29488

A general survey of the results of elastic stress analyses of cracked bodies is the basic objective of this work. The stress-intensity-factor method of representing results is stressed and compared with other similar methods. All three modes of crack surface displacements are considered, as well as specialized results applicable to plate and shell bending. Results for various media (e.g. anisotropic, viscoelastic or non-homogeneous) are contrasted with the analysis of homogeneous isotropic media. The accuracy of the representation of the crack tip stress fields by stress-intensity-factor methods is discussed pointing out some limitations of applicability. Methods of estimating and approximate analysis for stress-intensity-factors in complicated practical circumstances are also discussed.

author

STRESS ANALYSIS OF CRACKS

by Paul C. Paris*
and George C.M. Sih*

Introduction:

The redistribution of stresses in bodies caused by the introduction of a crack is one of the essential features which should be incorporated into an analysis of strength of structures with flaws. Moreover, the high elevation of stresses near the tip of a crack should receive the utmost attention, since it is at that point that additional growth of the crack takes place. As a consequence, it is the purpose of this paper to present a summary of current knowledge of crack tip stress fields and of the means of determination of the intensity of those fields.

Small amounts of plasticity and other non-linear effects may be viewed as taking place well within the crack tip stress field and hence may be neglected in this presentation of the gross features of those fields. It is the subject of other discussions to assess the effects caused by the fields, e.g. the plasticity within them and other requirements of formulation of a complete theory of fracture behavior.

* Associate Professor of Mechanics, Lehigh University,
Bethlehem, Pennsylvania

In his now famous paper Griffith [1] made use of the stress solution provided by Inglis [2] for a flat plate under uniform tension with an elliptical hole which could be degenerated into a crack. However, neither Griffith nor his predecessors had the knowledge of stress fields near cracks which is now available, so as a consequence, he devised an energy-rate analysis of equilibrium of cracks in brittle materials. Sneddon [3] was the first to give stress field expansions for crack tips for two individual examples, however, it was only later that Irwin [4,5] and Williams [6] recognized the general applicability of these field equations and extended them to the most general case for an isotropic elastic body [5]. It is this analysis to which initial attention shall be given.

Crack Tip Stress Fields for Isotropic Elastic Bodies

The surface of a crack, since they are stress free boundaries of the body near the crack tip, are the dominating influence on the distributions of stresses in that vicinity. Other remote boundaries and loading forces effect only the intensity of the local stress field.

The stress fields near crack tips can be divided into three basic types each associated with a local mode of deformation as illustrated in figure 1. The opening mode, I, is associated with local displacement in which the crack surfaces move directly apart (symmetric with respect to the x-y and x-z planes). The edge sliding mode, II, is characterized

by displacements in which the crack surfaces slide over one another perpendicular to the leading edge of the crack (symmetric with respect to the x-y plane and skew-symmetric with respect to the x-z plane). Mode III, tearing, finds the crack surfaces sliding with respect to one another parallel to the leading edge (skew-symmetric with respect to the x-y and x-z planes). The superposition of these three modes is sufficient to describe the most general case of crack tip deformation and stress fields.

The most direct approach to determination of the stress and displacement fields associated with each mode follows in the manner of Irwin [4,7], based on the method of Westergaard [8]. Modes I and II can be analyzed as plane extensional problems of the theory of elasticity which are subdivided as symmetric and skew-symmetric, respectively, with respect to the crack plane. Mode III can be regarded as the pure shear (or torsion) problem. Referring to figure 2 for notation, the resulting stress and displacement fields are (a full derivation is found in Appendix I):

Mode I

$$\begin{aligned}\sigma_x &= \frac{K_I}{\sqrt{2\pi r}} \cos \frac{\theta}{2} \left[1 - \sin \frac{\theta}{2} \sin \frac{3\theta}{2} \right] \\ \sigma_y &= \frac{K_I}{\sqrt{2\pi r}} \cos \frac{\theta}{2} \left[1 + \sin \frac{\theta}{2} \sin \frac{3\theta}{2} \right] \\ \tau_{xy} &= \frac{K_I}{\sqrt{2\pi r}} \sin \frac{\theta}{2} \cos \frac{\theta}{2} \cos \frac{3\theta}{2}\end{aligned}$$

$$\sigma_z = \nu(\sigma_x + \sigma_y), \quad \tau_{xz} = \tau_{yz} = 0 \quad (1)$$

$$\begin{aligned}u &= \frac{K_I}{G} \sqrt{\frac{r'}{2\pi}} \cos \frac{\theta}{2} \left[1 - 2\nu + \sin^2 \frac{\theta}{2} \right] \\ v &= \frac{K_I}{G} \sqrt{\frac{r'}{2\pi}} \sin \frac{\theta}{2} \left[2 - 2\nu - \cos^2 \frac{\theta}{2} \right]\end{aligned}$$

$$w = 0$$

Mode II

$$\begin{aligned}\sigma_x &= \frac{K_{II}}{\sqrt{2\pi r}} \sin \frac{\theta}{2} \left[2 + \cos \frac{\theta}{2} \cos \frac{3\theta}{2} \right] \\ \sigma_y &= \frac{K_{II}}{\sqrt{2\pi r}} \sin \frac{\theta}{2} \cos \frac{\theta}{2} \cos \frac{3\theta}{2} \\ \tau_{xy} &= \frac{K_{II}}{\sqrt{2\pi r}} \cos \frac{\theta}{2} \left[1 - \sin \frac{\theta}{2} \sin \frac{3\theta}{2} \right]\end{aligned}$$

(2)

$$\sigma_z = \nu(\sigma_x + \sigma_y), \quad \tau_{xz} = \tau_{yz} = 0$$

$$\begin{aligned}u &= \frac{K_{II}}{G} \sqrt{\frac{r}{2\pi}} \sin \frac{\theta}{2} \left[2 - 2\nu + \cos^2 \frac{\theta}{2} \right] \\ v &= \frac{K_{II}}{G} \sqrt{\frac{r}{2\pi}} \cos \frac{\theta}{2} \left[-1 + 2\nu + \sin^2 \frac{\theta}{2} \right]\end{aligned}$$

$$w = 0$$

Mode III

$$\tau_{xz} = - \frac{K_{III}}{\sqrt{2\pi r}} \sin \frac{\theta}{2}$$

$$\tau_{yz} = \frac{K_{III}}{\sqrt{2\pi r}} \cos \frac{\theta}{2}$$

(3)

$$\sigma_x = \sigma_y = \sigma_z = \tau_{xy} = 0$$

$$w = \frac{K_{III}}{G} \sqrt{\frac{2r}{\pi}} \sin \frac{\theta}{2}$$

$$u = v = 0$$

The equations (1) and (2) have been written for the case of plane strain (i.e. $w=0$) but can be changed to plane stress easily by taking $\sigma_z = 0$ and replacing the shear modulus, G , and Poisson's ratio, ν , in the displacements with appropriate values. These equations, (1), (2) and (3), have been obtained by neglecting higher order terms in r . Hence, they can be regarded as a good approximation in the region where r is small compared to other planar (x - y plane) dimensions of a body such as crack length and exact in the limit as r approaches zero.

The parameters, K_I , K_{II} , and K_{III} in the equations are stress-intensity-factors* for the corresponding three types of stress and displacement fields. It is important to notice that the stress-intensity-factors are not dependent on the coordinates, r and θ , hence they control the intensity of the stress fields but not the distribution for each mode. From dimensional considerations of equations (1), (2), and (3), it can be observed that the stress-intensity-factors must contain the magnitude of loading forces linearly for linear-elastic bodies and must also depend upon the configuration of the body including the crack size. Consequently, stress-intensity-factors may be physically interpreted as parameters which reflect the redistribution of stress in a body due to the introduction of a crack, and in particular they indicate the type (mode) and magnitude of force transmission through the crack tip region.

Elementary Dimensional Considerations for Determination of Stress-Intensity-Factors

An infinite plate subjected to uniform tensile stress, σ , into which a transverse crack of length, $2a$, has been introduced, is shown in figure 3. As a two dimensional problem of theory of elasticity only two characteristic dimensions are present, σ and a . Moreover, this configuration is symmetric with respect to the crack plane therefore only the first mode

* these stress-intensity-factors differ by a factor of $\sqrt{\pi}$ with earlier definitions of them.

fields are present. Then, simply from dimensional consideration [9] with equations (1), the only possibility is:

$$K_I = C_1 \sigma \sqrt{a} \quad (4)$$

$$K_{II} = K_{III} = 0$$

Hence, observations of symmetry and dimensional analysis can aid in determination of stress intensity factors. Though C_1 is undetermined by such considerations, later results will show it to be $\sqrt{\pi}$. However, even if C_1 is left undetermined the fracture size effect can be predicted for this configuration, since* as $K_I \rightarrow K_{Ic}$, then

$$\sigma \sqrt{a} = \text{const.} \quad (5)$$

By similar considerations of the plane extensional problem of a plate under shear, as shown in figure 4, the stress intensity factors are

$$K_{II} = \tau \sqrt{\pi a}$$
$$K_I = K_{III} = 0 \quad (6)$$

* $K_I \rightarrow K_{Ic}$, as a fracture criterion, is discussed in many other papers at this conference.

Moreover, analogous results may be obtained for the problem shown in figure 5, i.e. an infinity body with shear applied parallel to a tunnel crack of width, $2a$. They are:

$$K_{III} = \tau \sqrt{\pi a} \quad (7)$$

$$K_I = K_{II} = 0$$

Though these are relatively interesting examples, more complicated configurations are of practical importance, consequently, more powerful methods of analysis will be cited.

Stress-intensity-factors can be determined from the limiting values of elastic stress concentration factors [7] as the root radius, p , of the notch approaches zero. Consider a symmetrically loaded notch whereupon the tip will be embedded within a mode I stress field. The maximum stress, σ_0 will occur directly ahead of the notch. Again dimensional considerations of equations (1) lead to

$$K_I = C_2 \sigma_0 \sqrt{p} \quad (8)$$

in the limiting case the notch approaches a crack, as $p \rightarrow 0$, or

$$K_I = \lim_{p \rightarrow 0} \frac{\sqrt{\pi}}{2} \sigma_0 \sqrt{p} \quad (9)$$

The constant has been evaluated from equation (4) and the stress concentration solution for an elliptical hole in the

configuration shown in figure 3, which is:

$$\sigma_0 = \sigma \left(1 + 2 \sqrt{\frac{a}{p}}\right) \quad (10)$$

A multitude of stress concentration solutions available in the works of Neuber [10], Peterson [11], Savin [12], Isida [13] and others can be used to determine stress intensity factors for many configurations. Formulas corresponding to equation (9) can be as easily derived for modes II and III. They appear in Appendix II.

From the above dimensional considerations it is evident that the appearance of the $1/\sqrt{r}$ type of singularity in the stress field equations (1), (2) and (3) is a controlling feature in fracture size effects, the relationship of stress concentrations to stress intensity factors, and, as will be noted later, extension of fracture mechanics concepts to other than isotropic-elastic media.

Stress-Intensity-Factors from Westergaard Stress Functions

Several sources [4,5,7,8 and others] give Westergaard stress functions, Z , for crack problems. A discussion of the basic equations analysis of plane problems with this type of stress function is given in Appendix I.

For each of the three modes of crack tip stress fields the Westergaard stress function in the neighborhood of the crack tip takes the form

$$z = \frac{f(\zeta)}{\sqrt{\zeta}}, \quad \zeta = re^{i\theta} \quad (11)$$

where $f(\zeta)$ must be well behaved in that vicinity in order to ensure stress free crack surfaces*. Hence in the region close to the crack tip, i.e. $|\zeta| \rightarrow 0$, it is permissible to represent the stress function as [5]:

$$z \Big|_{|\zeta| \rightarrow 0} = \frac{f(0)}{\sqrt{\zeta}} \quad (12)$$

for mode I stress fields (see Appendix I). Comparing σ_y along the x-axis as computed from equation (12) and as given in equation (1) leads to:

$$K_I = \lim_{|\zeta| \rightarrow 0} \sqrt{2\pi\zeta} z_I \quad (13)$$

In a similar fashion for the other modes:

$$K_{II} = \lim_{|\zeta| \rightarrow 0} \sqrt{2\pi\zeta} z_{II} \quad (14)$$

$$K_{III} = \lim_{|\zeta| \rightarrow 0} \sqrt{2\pi\zeta} z_{III} \quad (15)$$

* Simple poles away from the crack tip will appear at locations of concentrated forces, etc.

As an example consider a plate with an infinite periodic array of cracks along a line with uniform tension, σ ; the half period is b and the half crack length a , as shown in figure 6. The stress function for this configuration is [4]:

$$Z_I = \frac{\sigma \sin \frac{\pi z}{2b}}{\left[\left(\sin \frac{\pi z}{2b} \right)^2 - \left(\sin \frac{\pi a}{2b} \right)^2 \right]^{1/2}} \quad (16)$$

In order to move the crack tip to the origin substitute $z = x+iy = a+\zeta$ and trigonometric identities, and eliminating terms of the order of ζ compared to terms of the order of a , the limiting process in equation (13) leads to:

$$K_I = \sigma \sqrt{\pi a} \sqrt{\frac{2b}{\pi a} \tan \frac{\pi a}{2b}} \quad (17)$$

$$K_{II} = K_{III} = 0$$

Referring to figure 6, the indicated axes of symmetry are lines devoid of shear stress, and subtracting a uniform normal stress, σ , in the horizontal direction (leads to no change in K_I) leaves only small self equilibrating normal stresses, σ_x , along these lines provided a is small compared to b . For these reasons it is regarded as permissible to cut the sheet along these lines and to use equation (17) as an approximate solution for finite width strips with central cracks provided a is less

than $b/2$. Results computed for strips by Isida [13] and Kobayashi [14,15], which are accurate to much larger relative values of a , indicate that this practice is sound (within 7%, see table I).

Similarly, cutting the problem in figure 6 along the y -axis and similar lines leads to an approximate solution, equation (17), for double edge notched strips which is acceptably accurate if a is greater than $b/2$ (within 2%). Bowie [16] has calculated results for edge notched strips which verify this accuracy.

The configuration shown in figure 6 with the applied stress, σ , replaced by in plane shear stress, τ , leads to:

$$Z_{II} = \frac{\tau \sin \frac{\pi z}{2b}}{\left[\left(\sin \frac{\pi z}{2b} \right)^2 - \left(\sin \frac{\pi a}{2b} \right)^2 \right]^{1/2}} \quad (18)$$

making use of equation (14) results in:

$$K_{II} = \tau \sqrt{\pi a} \sqrt{\frac{2b}{\pi a} \tan \frac{\pi a}{2b}} \quad (19)$$

$$(K_I = K_{III} = 0)$$

In a like fashion all results such as equations (16) and (17) for symmetric problems, mode I, are analogous to the corresponding

mode II problem equations (18) and (19) obtained by rotation of boundary forces and/or stresses through 90° in plane when treating extension of infinite plates, and certain other cases.

Moreover, the corresponding mode III problem, with the stress, σ , replaced by out of plane shear, τ , for a body of infinite extent in all directions, the stress function is identical to equation (18) and the stress-intensity-factor is:

$$K_{III} = \tau \sqrt{\pi a} \sqrt{\frac{2b}{\pi a} \tan \frac{\pi a}{2b}} \quad (20)$$

$$(K_I = K_{II} = 0)$$

It can be noted that the above examples of stress-intensity-factors from Westergaard stress functions, equations (17), (19) and (20), lead to the results in earlier examples, equations (4), (6) and (7), if b becomes very large compared to a .

Westergaard stress functions are available for many problems and with some experience it is easy to add solutions, but there are limitations to the scope of the method. The most serious drawback is that the method is normally restricted to infinite plane (two-dimensional) bodies with cracks along a single straight line. Another, more versatile approach to plane problems is available.

Stress-Intensity-Factors from General Complex Stress Functions

A complex stress function approach developed by Muskhelishvili [17] and others has some advantages over the Westergaard method by treating a broader class of plane extensional problems.

An Airy's stress function, ϕ , must satisfy the boundary conditions of a problem and the biharmonic equation, i.e. (see Appendix I)

$$\nabla^4 \phi = 0 \quad (21)$$

The general solution to equation (21) may be expressed as [17]

$$\phi = \text{Re} [\bar{z}\phi(z) + \chi(z)] \quad (22)$$

From this form for ϕ the sum of the normal stresses becomes

$$\sigma_x + \sigma_y = 4 \text{Re}[\phi'(z)] \quad (23)$$

Defining a complex stress-intensity-factor [18] by

$$K = K_I - i K_{II} \quad (24)$$

equations (1), (2), and (24) may be combined to give the same stress combination in the vicinity of a crack tip. The result is

$$\sigma_x + \sigma_y = \text{Re}\left[\frac{\sqrt{2}}{\sqrt{\pi r}} K\right] \quad (25)$$

for a crack tip at z_1 and for corresponding coordinate directions, i.e.

$$\zeta = z - z_1 \quad (26)$$

Substitution of equation (26) into (25) and comparing the result with equation (23) leads to

$$K = K_I - i K_{II} = 2 \sqrt{2\pi} \lim_{z \rightarrow z_1} \sqrt{z - z_1} \phi'(z) \quad (27)$$

The function $\phi(z)$ has been determined for a large number of crack problems [12, 17, 18, 19, 20], since with this technique conformal mapping of holes into cracks is permitted.

For a mapping function, $z = w(\eta)$, equation (27) becomes

$$K = 2 \sqrt{2\pi} \lim_{\eta \rightarrow \eta_1} \sqrt{w(\eta) - w(\eta_1)} \frac{\phi'(\eta)}{w'(\eta)} \quad (28)$$

The mapping of a crack of length, $2a$, into a circular hole of unit radius is given by

$$z = w(\eta) = \frac{a}{2} \left(\eta + \frac{1}{\eta} \right) \quad (29)$$

For this mapping equation (28) simplifies to

$$K = 2 \sqrt{\frac{\pi}{a}} \phi'(1) \quad (30)$$

The example of a single concentrated force, F , (per unit thickness) on a crack surface with arbitrary inclination, as

shown in figure 7, is solved by:

$$\phi'(n) = \frac{F a}{2\pi[a^2-b^2]^{1/2}} \left\{ -\frac{1}{n} + \left(\frac{n_0}{n_0-n}\right) \left[\left(\frac{1}{n}\right) - \left(\frac{1}{n_0+\frac{1}{n_0}}\right) \right] \right. \\ \left. + \left(\frac{1}{n_0-\frac{1}{n_0}}\right) \left[\frac{\kappa}{1+\kappa} \log n - \log(n_0-n) \right] \right\} \quad (31)$$

where n_0 corresponds to $z = b$, $F = P-iQ$, and κ is an elastic constant, which for plane strain is $\kappa = 3-4\nu$.

Using equation (30) with (31), the stress-intensity-factors are:

$$K_I = \frac{P}{2\sqrt{\pi a}} \left(\frac{a+b}{a-b}\right)^{1/2} + \frac{Q}{2\sqrt{\pi a}} \left(\frac{\kappa-1}{\kappa+1}\right) \\ K_{II} = \frac{-P}{2\sqrt{\pi a}} \left(\frac{\kappa-1}{\kappa+1}\right) + \frac{Q}{2\sqrt{\pi a}} \left(\frac{a+b}{a-b}\right)^{1/2} \quad (32)$$

The concentrated force solution, equations (32) provides the Green's functions to solve any single straight crack problem in an infinite plane from a knowledge of the stresses on the prospective crack surface with the crack absent, i.e. $\sigma_y(x,0)$ and $\tau_{xy}(x,0)$. The solution is

$$\begin{aligned}
K_I &= \frac{1}{\sqrt{\pi a}} \int_{-a}^a \sigma_y(x,0) \left(\frac{a+x}{a-x}\right)^{1/2} dx \\
K_{II} &= \frac{1}{\sqrt{\pi a}} \int_{-a}^a \tau_{xy}(x,0) \left(\frac{a+x}{a-x}\right)^{1/2} dx
\end{aligned} \tag{33}$$

In order to further illustrate the versatility of the complex stress function method, the problem of a crack of radius R , subtending an arc of angle, 2α , symmetrically with respect to the x -axis in an infinite sheet subjected to uniform biaxial tension may be treated, see figure 8. For this case Muskhelishvili [17] gives

$$\phi'(z) = \frac{\sigma \sqrt{R}}{2(1+\sin^2 \frac{\alpha}{2})} \left\{ \frac{z - \cos \alpha}{[1-2 \cos \alpha + z^2]^{1/2}} + \sin^2 \frac{\alpha}{2} \right\} \tag{34}$$

Relocation of a crack tip on the x -axis, as required by equation (27), may be accomplished by the substitution:

$$z = ie^{i\alpha} \cdot (\hat{z} - i - \sin \alpha \cos \alpha) \tag{35}$$

whereupon equations (27), (34) and (35) give

$$\begin{aligned}
K_I &= \frac{\sigma \sqrt{\pi R}}{(1+\sin^2 \frac{\alpha}{2})} \sqrt{\frac{\sin \alpha (1+\cos \alpha)}{2}} \\
K_{II} &= \frac{\sigma \sqrt{\pi R}}{(1+\sin^2 \frac{\alpha}{2})} \sqrt{\frac{\sin \alpha (1-\cos \alpha)}{2}}
\end{aligned} \tag{36}$$

Other notable examples of stress-intensity-factors for rather complicated cases of plane extension have been provided [18, 21, 22, 23, etc.] using this and similar methods. The power of this method for plane extension has been sufficiently illustrated, consequently, additional examples will be removed to Appendix II.

A similar complex variable approach has been developed to determine stress-intensity-factors in prismatic bars (with prismatic cracks) subjected to torsion and flexure [24, 25, 26]. This type of configuration leads to mode III stress-intensity-factors, some of which will also be tabulated in Appendix II.

Stress-Intensity-Factors for some Three-Dimension Cases

Using a method employing Fourier transforms, Sneddon [3] treated the case of a circular disk crack of radius, a , in an infinite solid subjected to uniform tension, σ , normal to the crack plane, see figure 9. His results for crack tip stress field expansions lead to:

$$K_I = \frac{2}{\sqrt{\pi}} \sigma \sqrt{a} \quad (37)$$

(by symmetry $K_{II} = K_{III} = 0$)

The analysis of stresses near ellipsoidal cavities in infinite bodies subjected to tension has been discussed by Sadowsky [27] and Green [28]. However, difficulties arise in the

stresses computed from their results near the crack edge when the ellipsoid is degenerated into a crack, see figure 10. Subsequently, Irwin [29] calculated the stress-intensity-factor at any location on the crack border, described by the angle, β , by comparing Green's results for displacements with equations (1). The formulas obtained are:

$$K_I = \frac{\sigma \sqrt{\pi a}}{\phi_0} \left(\sin^2 \beta + \frac{a^2}{b^2} \cos^2 \beta \right)^{1/4} \quad (38)$$

(by symmetry $K_{II} = K_{III} = 0$)

where ϕ_0 is the elliptic integral*

$$\phi_0 = \int_0^{\pi/2} \sqrt{1 - \left(\frac{b^2 - a^2}{b^2}\right) \sin^2 \theta} \, d\theta \quad (39)$$

Notice that for $b = \infty$, $\beta = \pi/2$ equations (38) and (39) reduce to equation (4) or for $b = a$ to equation (37), with corresponding changes from figure 10 to figure 3 or figure 9.

Though the above results for three dimensional problems are of extreme practical interest, the mathematical difficulty in attempting other such solutions is so great that a discussion of the possible methods would be of little interest.

* values of elliptic integrals are to be found in many mathematical tables.

However, in practical application of results it must be kept in mind that all bodies are really three dimensional and often the cracks which must be analyzed do not suit the idealized results exactly as presented here. Nevertheless, the results which are presented form the basis for sensible judgements from which three dimensional effects may be assessed. A later section on "Estimation of Stress Intensity Factors" will illustrate some use of that judgement.

Moreover, as a prime example of the fact that three dimensional effects are always present and yet may most often be justifiably neglected, consider sheet of finite thickness with a through-crack. If the sheet were infinitely thick plane strain would apply, or if infinitely thin then plane stress. But with finite thickness a mixed situation of plane stress near the surfaces of the plate and plane strain in the interior occurs in the crack tip stress field. Consequently, the stress intensity factors computed for plane problems represent only their values averaged through the thickness. Therefore, considering that plane stress vs. plane strain displacement fields differ by a factor of $(1-\nu^2)$, the actual values of stress intensity factors for a straight-through-crack can vary by $\sqrt{(1-\nu^2)}$ (or less) from the surface to the interior. The values at the surface being a maximum of 5% less than computed

values and correspondingly a maximum of 3% more in the interior (for $\nu = 0.3$). Though crack tip plasticity further complicates the situation, it is partially for this reason that the crack often begins to grow in the interior of a plate rather than at the surface to form a "tongue". Even though this effect is often observed, ignoring it leads to a desirable level of accuracy of computed values of stress-intensity-factors in developing fracture criteria*.

Edge Cracks in Semi-Infinite Bodies

The plane extensional problem of an edge notch, a , into a semi-infinite plane subjected to tension, σ , has been discussed by several authors [30, 31, 32, 16, etc.], see figure 11. Upon dimensional analysis leading again to equations (4) with C_1 left unknown, the task is merely to evaluate that constant. However, formidable methods must be employed to obtain the effect of the free surface of the half-plane. These methods use series-type mapping functions with the complex variable stress function method [16, 30] and/or dual integral equations resulting from a Green's function approach [31, 32]. The results may be computed to any desired degree of accuracy and (within

* So call "pop-in" tests actually make direct use of this effect.

1% of each other) they are:

$$K_I = 1.12 \sigma \sqrt{\pi a} \quad (40)$$

$$(K_{II} = K_{III} = 0)$$

Comparison of this result with either equation (4) or (17) leads to the conclusion that the free surface correction factor is 1.12 for edge notches perpendicular to uniform tension.

On the other hand for the analogous mode III case equation (7) and figure 5 with the introduction of a free surface perpendicular to the crack plane along the centerline of the crack, no correction is required [33, 26]. Therefore corresponding to figure 12 the stress intensity factor is:

$$K_{III} = \tau \sqrt{\pi a} \quad (41)$$

$$(K_I = K_{II} = 0)$$

There is no directly analogous mode II case corresponding to figures 11 or 12.

With these examples and their results the methods of determination of "closed form" stress-intensity-factors for some basic configurations have been illustrated. Subsequently, some other types of problems which have not lent themselves to closed form solutions bear discussion.

Two-Dimensional Problems of Plate Strips with Transverse Cracks

The class of two dimensional problems of plate strips with transverse internal, edge, and dual collinear edge cracks subjected to tension and in plane bending is of great practical interest for fracture testing procedures. However, closed form solutions for such problems are not available and many of the approximate solutions in the literature are of doubtful accuracy. Therefore it is important to not only cite these results but to give estimates of their accuracy.

The limitations on use of the so called "tangent" formula, equation (17), for centrally cracked strips and double edge notched strips subjected to tension were already discussed. The work cited [13, 14, 15, and 16] which evaluated those limitations was from direct attacks on the strip problems.

One of the most formidable approaches to this class of problems is found in the work of Isida, [13, 34, 35, 36, etc.]. Isida has extensively developed mapping functions for strip problems for determination of stress-concentrations at the tips of round ended cracks of end radius, p . His results are presented in the form [see 13]

$$\sigma_o = \sigma_{\max} = \frac{2 \sigma \sqrt{a}}{\sqrt{p}} f(\lambda) \quad (42)$$

where λ is the ratio of crack length to strip width. The function $f(\lambda)$ is obtained as a power series as a result of using power series mapping and stress functions. The form of equation (42) lends itself to direct substitution into equation (9) or alternately to techniques developed by Kobayashi [14]. The resulting stress-intensity factors can be computed to any degree of accuracy by Isida's methods, provided the power series employed in the analysis converge which they do for relatively large variations in λ . Within this minor limitation Isida's results lead to accuracies of within 1 or 2%.

Isida has computed results in the form of equation (42) for a variety of problems [13] of special interest in fracture testing such as the case of the centrally notched strip in tension, as shown in figure 13. Upon substitution of equation (42) into equation (9), it can be noted by comparing the result with equation (17) that $f(\lambda)$ corresponds to the exact correction factor for the stress intensity factor of a finite width strip whose approximate form is $\sqrt{\frac{2b}{\pi a} \tan \frac{\pi a}{2b}}$. Table I compares the two to illustrate the accuracy of equation (17).

Table I

$\lambda = \frac{a}{b}$	$\sqrt{\frac{2b}{\pi a} \tan \frac{\pi a}{2b}}$ (Equation 17)	$f(\lambda)$ (Isida [13])
0.074	1.00	1.00
0.207	1.02	1.03
0.275	1.03	1.05
0.337	1.05	1.09
0.410	1.08	1.13
0.466	1.11	1.18
0.535	1.15	1.25
0.592	1.20	1.33

Bueckner [37, 38] has developed integral equation procedures and solved many crack problems. He obtained the solution to a strip with a single edge notch subjected to bending, see figure 14, which is conveniently reported in [39]. The results so reported obviously lack the correction factor for a free surface, for small crack sizes discussed in conjunction equation (40), which is a 12% error. However, as noted following equation (17), the effect of the crack's emanation from a free edge disappears with deepening cracks consequently the error should diminish. The results are expressed as follows:

$$K_I = \frac{6M}{(h-a)^{3/2}} g\left(\frac{a}{h}\right) \quad (43)$$

$$(K_{II} = K_{III} = 0)$$

where $g\left(\frac{a}{h}\right)$ is given in table II.

Table II

a/h	0.05	0.1	0.2	0.3	0.4	0.5	0.6	(and larger)
g(a/h)	0.36	0.49	0.60	0.66	0.69	0.72	0.73	

The values in Table II suit the limiting case of deep notches as determined from Neuber's results [10]. Therefore it might be presumed that Table II reports values with errors of far less than 12% for a/h greater than 0.2. However, several recent papers on notch bending analysis disagree widely with the values in Table II and though these recent results claim agreement with "compliance calibrations" for a/h in the normal testing range, they do not agree with results for either of the limiting cases, shallow or deep notches. Consequently, the matter of accuracy of the notched bending analysis is left unresolved at this time.

Bowie developed polynomial mapping functions for use with the complex stress function technique to solve plane problems, such as cracks emanating from circular holes [40] and the double edge notched strip in tension [16]. The latter example, as illustrated in figure 15, provides an indication of the validity of employing equation (17) for this configuration. Comparing Bowie's results with equation (17) is most lucidly accomplished

using a correction factor $h(a/b)$ on equation (17) or

$$K_I = \sigma \sqrt{\pi a} \sqrt{\frac{2b}{\pi a} \tan \frac{\pi a}{2b}} h(a/b) \quad (44)$$

$$(K_{II} = K_{III} = 0)$$

for which his computed values are given in Table III*.

Table III

a/b	$h(a/b)$ ($\frac{L}{b} = 1.00$)	$h(a/b)$ ($\frac{L}{b} = 3.00$)	$\sqrt{\frac{2b}{\pi a} \tan \frac{\pi a}{2b}} h(a/b)$ ($\frac{L}{b} \rightarrow \infty$)
0.1	1.13	1.12	1.12
0.2	1.13	1.11	1.12
0.3	1.14	1.09	1.13
0.4	1.16	1.06	1.14
0.5	1.14	1.02	1.15
0.6	1.10	1.01	1.22
0.7	1.02	1.00	1.34
0.8	1.01	1.00	1.57
0.9	1.00	1.00	2.09

From Table III it can be immediately observed that for low a/b values the correction factor of 1.12 for a crack from a free surface, as illustrated by equation (40), is present.

* The last column in Table III agrees within 1% with a similar formula proposed by G. R. Irwin on the basis of estimating the various effects. It is

$$K_I = \sigma \sqrt{\pi a} \left[\frac{2b}{\pi a} \left(\tan \frac{\pi a}{2b} + 0.1 \sin \frac{\pi a}{b} \right) \right]^{1/2}$$

As a/b increases its effect disappears and equation (17) applies as noted previously. The last column of Table III combines the two effects, i.e. the free surface and the finite width strip, to give the complete correction factor (within 1%) for all values of a/b . From this study it can be noticed that using equation (40) for $a/b < 0.5$ and equation (17) for $a/b > 0.5$ results in errors of less than 3% for the configuration shown in figure 15 provided $L/b > 3$. As a consequence it has been illustrated that basic solutions like equations (17) and (40) can often be used with proper judgement to provide approximate analyses of more difficult situations like figure 15.

Collocation procedures for strips of finite length have been developed by Kobayashi [15] and Gross [41]. As an example of the method Kobayashi treated the strip configuration in figure 13 using the general complex stress functions of Muskhelishvili [17], collocating equally spaced points on the sides and ends of the strip. He observed agreement within about 5% of Isida's results as given in Table I.

Gross treated the single edge notched strip using William's [6] eigenfunction representation of the Airy stress function. The configuration is shown in figure 16. He found that collocation at 20 or more boundary points was required to obtain convergence. His results can be stated in the form:

$$K_I = \sigma \sqrt{a\pi} k\left(\frac{a}{b}\right) \quad (45)$$

$$(K_{III} = K_{III} = 0)$$

where $k\left(\frac{a}{b}\right)$ is given as a correction factor for this strip problem in Table IV.

Table IV

a/b	k(a/b) (Gross [41])	$\sqrt{\frac{2b}{\pi a} \tan \frac{\pi a}{2b}}$	k(a/b) (Bowie [16])
		• h(a/b) (from Table III, and equation (44))	
0.10	1.14	1.12	1.14
0.20	1.19	1.12	1.15
0.30	1.29	1.13	1.18
0.40	1.37	1.14	1.22
0.50	1.50	1.15	1.31
0.60	1.66	1.22	1.46
0.70	1.87	1.34	1.67
0.80	2.12	1.57	1.95
0.90	2.44	2.09	2.25
1.00	2.82	-	2.58

By comparison of Gross's results (figure 16) with Bowie's double edge notch results (figure 15), columns 2 and 3 of Table IV, the apparently large influence of bending due to the lack of

symmetry in the single edge notch case is observed. Gross's results reportedly agree with experimentally measured values (i.e. compliance measurements) within a few percent for $0.40 < a/b < 1.00$. However, new results by Bowie [16] shown in column 4 leave the matter of accuracy in doubt for this configuration.

Following the procedures of Kobayashi and Gross, it is a straight forward matter to solve additional problems. Moreover, similar numerical procedures based on collocation of boundary conditions in the mean, using other representations of the Airy stress function, and/or energy methods are available for development.

Reinforced Plane Sheets

Many conventional structures are fabricated from plane sheets (plates) with reinforcing stiffeners or doubler plates attached by riveting, welding and other means. Often the attachments are designed as crack arrestors in order to provide so called "fail safe" structures.

In order to analyze some of these configurations it is appropriate to determine stress-intensity-factors for cracks in sheets with stiffeners perpendicular to the cracks. Romualdi [42, 43] and Paris [44, 45] provided some early solutions to

estimate the effect of rivet forces tending to hold a crack closed. Sanders [46] discussed the problem of action of an integral stiffener crossing the center of a cracks. Isida [13, 47] extended his methods to give results for centrally cracked strips with integrally reinforced edges and to infinite sheets with a periodic array of cracks along a line with interspersed integral stiffeners. Greif [48] has solved the problem of a single crack and an integral stiffener (passing outside the crack) in an infinite sheet, and in a continuation of that work the riveted stiffener has been treated [49]. Moreover, Terry [50] has analyzed some similar riveted and welded stiffener problems, as an extension of work by Erdogan [21]. Cracks within one sheet of a riveted doubler plated area of a structure were treated by Paris [44]. Many of the results of these analyses will be tabulated in Appendix II. Since, this class of problems is difficult to formulate, the methods employed are rather obtuse and specialized. Consequently, they will not be described here other than to remark that the most general approaches available are those of Isida [13], Greif [48] and Terry [50].

Thermal Stresses

It has been shown that the crack tip stress field equations for isotropic bodies, equations (1), (2) and (3) also

provide the proper field equations for thermal stress states [51], (with the unlikely exception of the crack tip as a point source of heat). Therefore the concept of stress intensity factors is in general applicable to thermal stress problems.

As an example consider the case of uniform heat flow in a sheet, with an undisturbed temperature gradient, ΔT , at an angle β with respect to a crack of length, $2a$, acting as an insulator, as shown in figure 17. Florence and Goodier [52] have provided the complex stress function for this configuration. It is:

$$\phi(\eta) = \frac{iE\alpha a^2 \Delta T}{8} \sin \beta \log \eta \quad (46)$$

as a consequence of similarity of the resulting crack tip stress field equation with ordinary (isothermal) plane extension, equations (29) and (30) may be applied to equation (46) which results in:

$$K_{II} = \frac{E\alpha a^{3/2} \Delta T}{4} \sin \beta \quad (47)$$

$$(K_I = K_{III} = 0)$$

where α is the coefficient of thermal expansion and E is Young's modulus. Other examples, [51], will be cited in Appendix II.

Stress Intensity Factors for the Bending of Plates and Shells

The field equations for the stresses near a sharp notch in a plate subjected to bending was first considered by Williams [53, 54] who later applied like methods to a more detailed discussion of cracks [55]. Using the classical, Kirchhoff theory of plate bending he obtained the following stress field equations, see figure 18:

$$\begin{aligned} \sigma_r &= \frac{(7+\nu)}{2(3+\nu)} \frac{K_B}{\sqrt{2\pi r}} \frac{z}{h} \left[\frac{(3+5\nu)}{(7+\nu)} \cos \frac{\theta}{2} - \cos \frac{3\theta}{2} \right] \\ &+ \frac{(5+3\nu)}{2(3+\nu)} \frac{K_S}{\sqrt{2\pi r}} \frac{z}{h} \left[-\frac{(3+5\nu)}{(5+3\nu)} \sin \frac{\theta}{2} + \sin \frac{3\theta}{2} \right] \\ \sigma_\theta &= \frac{(7+\nu)}{2(3+\nu)} \frac{K_B}{\sqrt{2\pi r}} \frac{z}{h} \left[\frac{(5+3\nu)}{(7+\nu)} \cos \frac{\theta}{2} + \cos \frac{3\theta}{2} \right] \\ &- \frac{(5+3\nu)}{2(3+\nu)} \frac{K_S}{\sqrt{2\pi r}} \frac{z}{h} \left[\sin \frac{\theta}{2} + \sin \frac{3\theta}{2} \right] \\ \tau_{r\theta} &= \frac{(7+\nu)}{2(3+\nu)} \frac{K_B}{\sqrt{2\pi r}} \frac{z}{h} \left[-\frac{(1-\nu)}{(7+\nu)} \sin \frac{\theta}{2} + \sin \frac{3\theta}{2} \right] \\ &+ \frac{(5+3\nu)}{2(3+\nu)} \frac{K_S}{\sqrt{2\pi r}} \frac{z}{h} \left[-\frac{(1-\nu)}{(5+3\nu)} \cos \frac{\theta}{2} + \cos \frac{3\theta}{2} \right] \end{aligned}$$

where the constants in Williams' analysis [55] have been modified in order to define [18, 56] the plate bending and plate shearing stress-intensity-factors, K_B and K_S , in a manner consistent with (but not quite corresponding to) the first and second mode types, K_I and K_{II} , respectively, as defined by equations (1) and (2). Though polar instead of rectangular stress components are given for compactness in equations (48), the similarity of these results with equations (1) and (2) is immediately apparent. This similarity is further clarified upon computing K_B and K_S for some configurations and loadings of interest.

The governing equation for free bending of plates (no transverse loads) by the Kirchhoff theory is:

$$\nabla^4 w = 0 \quad (49)$$

where w is the transverse displacement. Consequently, an analysis [18] ensues of an identical nature to equations (21) through (27) which gives:

$$K_B - i K_S = - \frac{\sqrt{2\pi E} h(3+\nu)}{(1-\nu^2)} \lim_{z \rightarrow z_1} \sqrt{z-z_1} \phi'_B(z) \quad (50)$$

where $\phi_B(z)$ is the plate bending stress function discussed extensively by Savin [12].

Furthermore, mapping is again permitted or as equation (30) followed from (27), for the mapping function given by equation (29), equation (50) becomes

$$K_B - i K_S = -\sqrt{\frac{\pi}{a}} \frac{E h(3+\nu)}{(1-\nu^2)} \phi'_B(1) \quad (51)$$

For the example of an infinite plate subjected to uniform moment, M_o , all around the boundary, and with a crack of length, $2a$, as in figure 19, Savin [12] gives the stress function,

$$\phi_B(\eta) = -\frac{M_o a(1-\nu)}{E h^3} \left[\eta + \frac{(1-\nu)}{(3+\nu)} \frac{1}{\eta} \right] \quad (52)$$

Using equation (51) and (52) the result is:

$$K_B = \frac{6 M_o}{h^2} \sqrt{\pi a} \quad (53)$$

$$(K_S = 0)$$

Since the stress in the surface layer of the plate, σ_o , away from the crack is

$$\sigma_o = \frac{6 M_o}{h^2} \quad (54)$$

the analogy between equations (53) and (4) is evident.

Moreover, Erdogan [56] has shown experimentally that in brittle materials (like plexiglass) the fracture mechanics concept of K_B reaching a critical value K_{BC} is appropriate and analogous to the extensional first mode case, i.e. K_{Ic} . Incidentally, Erdogan [57] also shows that the critical value of stress intensity factors applies to the extension second mode, i.e. K_{IIc} , which again is shown to be analogous to the shear case of bending, i.e. K_{Sc} . Consequently, the plate bending and shearing stress intensity factors as defined in equations (48) are of some immediate practical interest.

However, equations (1), (2) and (3) were purported to give all tip stress fields for elastic bodies and yet the field for plate bending as predicted by equations (48) are not identical to them. This is because the classical Kirchhoff theory of bending is an approximate theory which does not take into account the details of the stress distribution near boundaries or discontinuities in the plate. The crack tip and crack surface boundaries are locations where details are not clear.

Subsequently, Knowles [58] pointed out that using Reissner's [59] more accurate plate theory leads to a correction of equations (48) which on the surface of the plate makes them

identical to equations (1) and (2) except for a constant factor. Moreover, the character and role of K_B and K_S are preserved through this correction. Hence, it is concluded that they are directly proportional to (completely analogous to) their counterparts K_I and K_{II} where elastic action is concerned. Williams [60] pointed this out in reference to the experiments by Erdogan [56]. This correspondence has also been observed for fatigue crack growth [61].

Therefore, both theoretical and experimental results for fracture tests have led to:

$$K_B = \frac{(3+\nu)}{(1+\nu)} K_I \quad (55)$$

on the surface of the plate. The sensibility of use the Kirchhoff theory to compute K_B values is also clear when it is reasoned that the values of stress intensity factors reflect the intensity of general transmission of applied loads into the crack tip region. The general properties of gross load transmission are unaffected by the boundary layer of about one plate thickness, h , in which the Reissner theory applies. Consequently, equation (55) is always correct for converting Kirchhoff theory stress intensity factors, K_B , to the Reissner theory result, K_I , for a given configuration.

Several solutions for K_B and K_S are now available [18] and others can be obtained in a direct fashion using equations (50) or its equivalent for other types of stress functions. Some of the available results will be tabulated in Appendix II.

The case of general bending and extension of thin shells with cracks has been shown by Sih [62] to give crack tip stress fields equivalent to combining modes I and II with the bending fields, i.e. equations (1) and (2) and equation (48). Modes I and II result from extension of the middle surface of the shell and the bending fields result from changes in the curvature of the middle surface. Consequently, the stress intensity factor concept is also of general applicability to shells.

However, computing the values of the stress intensity factors for particular configurations in shells is very difficult.

Moreover, it may be observed [62] that the extension and bending effects in shells will be coupled, so that the stress intensity factors resulting from solutions must reflect this coupling. As a consequence of the coupling, formulas for stress intensity factors will involve many parameters (coupling terms) so that they will, to say the least, be complicated.

Folias [63, 64] and Ang [65], noting the similarity of equations for plates on elastic foundations and shallow

spherical shells [66], have attempted some problems in these areas. However, no other attempts at the complete solutions to shell problems are known.

On the other hand some parametric studies of possible shell effects on cracks in cylinders have been attempted in several articles [67, 68, 69, 70]. The results indicate that the experimental data on failure of cracked shells can in fact be correlated in terms of elastic shell parameters. Hence, it is hopeful that further progress can be made soon toward quantitative prediction of shell effects on an analytical basis.

The problem of crack arrestor rings on shells is at least another degree more difficult. Nevertheless, since this problem is of prime interest in tear resistant design, efforts are being made toward empirical methods of design [69, 71]. The complete analytical solution to such a problem is as yet improbable.

Couple Stress Problems with Cracks

Another area analogous to shell problems through having similar governing equations is that of couple stresses [72, 73]. The formulation of couple stress problems takes into account the gradients of stresses in terms of couples on infinitesimal elements in order to account for the effects of lattice curvature in crystals, etc. Setzer [74] has shown that for

extension of cracked plates due to uniform applied stress away from the crack, no modification in the field equations (1), or the stress intensity factors, for example equation (4), is required. However, where the applied stresses away from the crack possess gradients, the values of stress intensity factors will be modified by factors of the form

$$\left[1 + A_1 \left(\frac{\lambda}{a}\right) + A_2 \left(\frac{\lambda}{a}\right)^2 + A_3 \left(\frac{\lambda}{a}\right)^3 + \dots \right] \quad (56)$$

where λ is a couple stress (lattice) parameter or characteristic length of the material. The A_i are of the order of unity or smaller and λ is of the order of lattice dimensions, consequently these results would be of a greatest interest in analyzing fine cracks in crystals, except for the fact that the methods involved are similar to and may be carried over to the analysis of shells.

Estimation of Stress Intensity Factors for Some Cases of Practical Interest

Armed with the principles of linear elastic theory, such as "the principle of superposition", etc. and with an intuitive grasp of a "strength of materials" approach, it is possible to form estimates of stress intensity factors. This was made partially evident in the case of an embedded

elliptical crack in the discussion of limiting cases following equation (38) and (39). Other situations where limiting cases of different problems are comparable were illustrated in Table I, III and IV and examples in the text. Notice especially, as in these tables, that one problem solution often forms an upper or lower bound on the solution of others. These concepts will be employed in examples of estimating to follow.

Consider the configuration of a notched round bar with an outside diameter, D , and notched section diameter, d , and subjected extension causing a net section stress, σ_{net} . See figure 20. From dimensional considerations and symmetry, it is noted that the stress intensity factor may be stated in the form,

$$K_I = \sigma_{net} \sqrt{\pi D} F(d/D) \quad (57)$$

$$K_{II} = K_{III} = 0$$

where $F(d/D)$ is an unknown dimensionless function of the diameter ratio. The end values (i.e. $d/D \rightarrow 0$ or 1.0) of the function can be established by examining limiting cases.

As $D \rightarrow \infty$ dimensional analysis leads to

$$K_I = C_3 \sigma_{net} \sqrt{\pi d} \quad (58)$$

thus, for small values of d/D ,

$$F_u(d/D) = C_3 \sqrt{\frac{d}{D}} \quad (59)$$

the value of C_3 is found to be $\frac{1}{2\sqrt{2}}$ using equation (9) and the stress concentration solution for the problem given by Neuber [10] and Peterson [11]. Since the free surface introduced by the finite diameter of the bar lowers the stress intensity factor, $F_u(d/D)$ is an upper bound on $F(d/D)$ for all values of d/D .

On the other hand for $d/D \rightarrow 1$ Bowie's solution for the double edge notched sheet, equation (44), simulates the problem upon substituting

$$a = \frac{D}{2} \left(1 - \frac{d}{D}\right)$$

$$\frac{a}{b} = 1 - \frac{d}{D}$$

and

$$\sigma = \sigma_{\text{net}} \left(\frac{d}{D}\right)^2 \quad (60)$$

The result conforms with equation (57), i.e.

$$K_I = \sigma_{\text{net}} \sqrt{\pi D} \left[\left(\frac{d}{D}\right)^2 \sqrt{\frac{1}{\pi} \tan \frac{\pi}{2} \left(1 - \frac{d}{D}\right) h \left(1 - \frac{d}{D}\right)} \right] \quad (61)$$

consequently,

$$F_L\left(\frac{d}{D}\right) = \left(\frac{d}{D}\right)^2 \sqrt{\frac{1}{\pi} \tan \frac{\pi}{2}\left(1-\frac{d}{D}\right)} h\left(1-\frac{d}{D}\right) \quad (62)$$

where $h(\)$ is as tabulated in Table III. This function $F_L\left(\frac{d}{D}\right)$ is a lower bound on $F(d/D)$ for all values of d/D , since the curvature of the bar causes increased crack tip stress over the flat plate solution as d/D recedes from the value 1.

Finally from Peterson's [11] stress concentration values and equation (9), and other considerations, the maximum value of $F(d/D)$ is estimated to be 0.240. Interpolating between these solutions results in the estimation values in Table V.

Table V

d/D	$F_L(d/D)$	$F_u(d/D)$	$F(d/D)$
0	0	0	0
0.1	-	0.111	0.111
0.2	0.046	0.158	0.155
0.3	-	0.194	0.185
0.4	0.118	0.223	0.209
0.5	-	0.250	0.227
0.6	0.185	0.274	0.238
0.65	0.203	-	0.240
0.70	0.217	0.296	0.240
0.75	0.226	-	0.237
0.80	0.230	0.317	0.233
0.85	0.224	-	0.225
0.90	0.205	0.336	0.205
0.95	0.162	-	0.162
0.97	0.130	-	0.130
1.00	0	0.353	0

By making use of careful judgement of the limits of applicability of the limiting cases, equations (59) and (62) and the analysis of stress concentration [11], the accuracy of $F(d/D)$ in Table V can be stated with confidence. From d/D of 0 to 0.4, it is $\pm 3\%$; from d/D of 0.4 to 0.85, it is $\pm 5\%$; and from d/D of 0.85 to 1.0, it is $\pm 2\%$. Therefore, a solution with sufficient precision for practical applications has been constructed.

This configuration is often used for fracture testing and a simplified formula is employed, i.e. [75],

$$K_I = 0.233 \sigma_{\text{net}} \sqrt{\pi D} \quad (63)$$

This formula seems most reasonable since 0.233 agrees with the values of $F(d/D)$ in Table V within 5% over the range of d/D from 0.48 to 0.86. Further improvements in the accuracy of the values given would require a full analysis of the problem, such as suggested by Sneddon [76] or Bueckner [77].

Another configuration, which has been discussed by Irwin [29], is that of a semi-elliptical surface crack in a plate, see figure 21. This configuration is both typical of flaws and is used in fracture testing (simulating this type of flaw). If the plate is subjected to general uniform extension by stresses, σ , σ' and τ ; the stress, σ' , parallel to the crack

causes no singularity or no contribution to stress intensity factors. Consequently σ' will be ignored.

If b/a is large and a/t small compared to one, the stress intensity factors at the end of the semi-minor axis, a , can be estimated from equations (17) and (20), making use of free-edge corrections as in equations (40) and (41). Then, the correction ϕ in equations (38) and (39) should be applied as b/a values are reduced toward one. However, the free edge correction probably diminishes as b/a approaches one and the tangent correction in equations (17) and (20) is also an overcorrection in that limit. On the other hand equations (44) and (45) and Table IV show that single edge notches induce bending which increases the stress intensity factor, but less so in this case since the uncracked portion of the plate would inhibit bending. Finally, Table I shows the underestimation of the tangent correction as a/t becomes larger. Taking all these factors into account, equations (17), (20), (38), (39), (40), (41), (42), (44) and (45), and their considerations lead to the approximations:

$$\begin{aligned}
 K_I &= \left[1 + 0.12\left(1 - \frac{a}{b}\right)\right] \frac{\sigma \sqrt{\pi a}}{\phi_0} \sqrt{\frac{2t}{\pi a} \tan \frac{\pi a}{2t}} \\
 K_{II} &= 0 \\
 K_{III} &= \frac{\tau \sqrt{\pi a}}{\phi_0} \sqrt{\frac{2t}{\pi a} \tan \frac{\pi a}{2t}}
 \end{aligned} \tag{64}$$

for the stress intensity factors at the end of the semi-minor axis, a . For the ranges of b/a from one to ten or more and of a/t from zero to one-half the accuracy is within about $\pm 5\%$. Moreover, for b/a up to about five and a/t up to three-fourths the accuracy is still probably better than $\pm 10\%$, considering all the compensating errors. This case has at least provided a classic example of estimating methods using many other solutions for stress intensity factors to treat an important problem which is all but impossible to solve directly.

A word of warning with complicated cases like equations (64) is in order. If the crack tip plasticity subtends a major portion (say one-half) of the distance between the crack front and the back side of the plate, use of these equations would become indeed doubtful. Moreover, estimation of the amount of plasticity is clearly more complicated here than in other situations, but surely possible. Such estimates are beyond the scope of this discussion and the reader is referred to [78]. Moreover, in passing it is note-worthy that restrictions on crack tip plastic zone sizes are always present in making direct applications of the elastic analyses [75]. For certain situations estimated corrections to the analysis for crack tip plasticity effects have been proposed [44, 75, 78, etc.].

Estimates can be made for stress intensity factors for

quite arbitrary crack front contours in three-dimensional bodies subjected to uniform tension, σ , perpendicular to the crack plane in the region including the whole crack. Consider the embedded crack whose plan view is shown in figure 22. Using the previous results for circular disk cracks, equation (37), and for tunnel cracks, equation (4), bounds can be established on the crack front for various portions of the contour, where

$$K_I = K_1 \text{ or } K_2 \text{ or } K_3 \text{ or } K_4$$

$$K_{II} = 0 \quad (65)$$

$$K_{III} = 0$$

The value of K_1 will be slightly greater than that for a disk crack of radius, a_1 , but far less than a tunnel crack of width, $2a_1$. Therefore from equations (4) and (37),

$$\frac{2}{\pi} \sigma \sqrt{\pi a_1} < K_1 \ll \sigma \sqrt{\pi a_1} \quad (66)$$

Since $\frac{2}{\pi}$ is about 0.64, if K_1 is guessed to be

$$K_1 \approx 0.75 \sigma \sqrt{\pi a_1} \quad (67)$$

The result is surely within $\pm 10\%$ along the whole portion of the contour marked, K_1 , in figure 22. Now, K_2 is closer to the

tunnel crack case or a guess is

$$K_2 \approx 0.85 \sigma \sqrt{\pi a_1} \quad (68)$$

the neck of width, $2a_3$, makes K_3 slightly higher than the comparable tunnel crack or

$$K_3 \approx 1.05 \sigma \sqrt{\pi a_3} \quad (69)$$

and similar to K_1 , the guess for K_4 is

$$K_4 \approx 0.75 \sigma \sqrt{\pi a_4} \quad (70)$$

These estimates are surely all correct within $\pm 10\%$ (and probably $\pm 5\%$). Moreover, additional refinements are possible, such as noting that K_3 on the upper part of the contour is likely about 5% less than on the lower contour in figure 22, due to the curvature of the centerline of the neck, $2a_3$.

Corrections can also be added for the proximity to a free surface, such as the tangent correction in equation (17), or for the emanation of the crack from a free surface, such as equation (40). The method of estimating has now been sufficiently illustrated to allow direct application to a multitude of examples. In order to develop confidence in estimating procedures, it is suggested that one may, for example, estimate the stress intensity factor values for an

elliptical crack using the above procedure, equations (66) through (70), and compare the results with the exact values, equation (38).

Stress Fields and Intensity Factors for Homogeneous Anisotropic Media

An interest in stress analysis of cracks for various media, such as anisotropic, visco-elastic, and/or non-homogeneous materials, stems from two motivations. First, the effects of slight amounts of directionality, creep and inhomogeneity on the stress distribution and intensity are useful in assessing the limits of applicability of the conceptual model of fracture mechanics based on linear-elastic theory. In addition studies of the stress analysis of these various types of media will provide the basis of extension of fracture mechanics to such materials.

Several authors have treated special cases of crack problems in anisotropic media, such as orthotropy [32, 79, 80] or particular configurations [81, 82]. However, the general anisotropic case can be treated in order to determine crack tip stress fields and to define intensity factors in a manner completely analogous to equations (1), (2) and (3). The

methods discussed extensively by Lekhnitzki [83] will be employed here.*

The Hooke's law for a homogeneous (rectilinearly) anisotropic material is:

$$\begin{aligned}
 \epsilon_x &= a_{11} \sigma_x + a_{12} \sigma_y + a_{13} \sigma_z + a_{14} \tau_{yz} + a_{15} \tau_{xz} + a_{16} \tau_{xy} \\
 \epsilon_y &= a_{21} \sigma_x + \dots \\
 \epsilon_z &= a_{31} \sigma_x + \dots \\
 \gamma_{yz} &= a_{41} \sigma_x + \dots \\
 \gamma_{xz} &= a_{51} \sigma_x + \dots \\
 \gamma_{xy} &= a_{61} \sigma_x + a_{62} \sigma_y + a_{63} \sigma_z + a_{64} \tau_{yz} + a_{65} \tau_{xz} + a_{66} \tau_{xy}
 \end{aligned}$$

where from reciprocity $a_{ij} = a_{ji}$ (71)

Referring to figure 2 for the coordinates and notation with respect to a crack front, the crack tip stress fields may be resolved from two cases of plane problems which are defined as:

(1) Plane strain, i.e. $\frac{\partial u}{\partial z} = \frac{\partial v}{\partial z} = w = 0$

or $\epsilon_z = \gamma_{yz} = \gamma_{xz} = 0$

(2) Pure shear, i.e. $u = v = \frac{\partial w}{\partial z} = 0$

or $\epsilon_z = \epsilon_x = \epsilon_y = \tau_{xy} = 0$

The superposition of results from these plane problems will

* The mathematical derivation of stress fields leading to equations (81) through (85) etc. are not a requirement of useful interpretation of those results.

allow treatment of the general case of crack tip stress fields similar to equations (1), (2) and (3).

(1) Plane Strain: For this case the Hooke's law may be reduced, using the restrictions on strain to eliminate the appearance of z-components of stress, to give:

$$\begin{aligned}\epsilon_x &= A_{11} \sigma_x + A_{12} \sigma_y + A_{16} \tau_{xy} \\ \epsilon_y &= A_{21} \sigma_x + A_{22} \sigma_y + A_{26} \tau_{xy} \\ \gamma_{xy} &= A_{61} \sigma_x + A_{62} \sigma_y + A_{66} \tau_{xy}\end{aligned}\tag{72}$$

where again $A_{ij} = A_{ji}$ and the A_{ij} can be expressed in terms of a_{ij} directly if desired. Using an Airy stress function, U , with stress components defined as the usual second derivatives, equilibrium is automatically satisfied and the compatibility equations lead to:

$$D_1 \cdot D_2 \cdot D_3 \cdot D_4 \cdot U = 0\tag{73}$$

where

$$D_k = \frac{\partial}{\partial y} - \mu_k \frac{\partial}{\partial x}$$

and μ_k are the roots of

$$A_{11} \mu^4 - 2 A_{16} \mu^3 + (2 A_{12} + A_{66}) \mu^2 - 2 A_{26} \mu + A_{22} = 0\tag{74}$$

These elastic constants, μ_k , are complex or pure imaginary and occur in conjugate pairs [83], i.e. $\mu_3 = \bar{\mu}_1$ and $\mu_4 = \bar{\mu}_2$.

Defining the complex variables z_1 and z_2 by

$$\begin{aligned} z_1 &= x + \mu_1 y \\ z_2 &= x + \mu_2 y \end{aligned} \tag{75}$$

the general solution to equation (73) can be written, if

$$\mu_1 = \mu_2$$

$$\begin{aligned} U &= U_1(z_1) + \bar{z}_1 U_2(z_1) + \\ &+ U_3(\bar{z}_1) + z_1 U_3(\bar{z}_1) \end{aligned}$$

or if

$$\mu_1 \neq \mu_2$$

$$\begin{aligned} U &= U_1(z_1) + U_2(z_2) + \\ &+ U_3(\bar{z}_1) + U_4(\bar{z}_2) \end{aligned} \tag{76}$$

and with the further restriction that U must be real they become

$$U = 2 \operatorname{Re}[U_1(z_1) + \bar{z}_1 U_2(z_1)]$$

or

$$U = 2 \operatorname{Re}[U_1(z_1) + U_2(z_2)] \tag{77}$$

The similarity of the first case of equation (77) with equation (22) is appropriate since for isotropic media, $\mu_1 = \mu_2 = i$. Therefore, the orthotropic case with the crack on a principal plane which leads to $\mu_1 = \mu_2$ has been reduced to the

same case as isotropic elasticity with the simple change of variable $z_1 = x + \mu_1 y$. The more general case of anisotropy, the second of equations (77) or $\mu_1 \neq \mu_2$ will follow in the remaining discussion.

The stress and displacement components are found from the Airy stress function, \mathcal{U} , by the usual combination of derivatives which give:

$$\sigma_x = 2 \operatorname{Re}[\mu_1^2 \mathcal{U}_1''(z_1) + \mu_2^2 \mathcal{U}_2''(z_2)]$$

$$\sigma_y = 2 \operatorname{Re}[\mathcal{U}_1''(z_1) + \mathcal{U}_2''(z_2)]$$

$$\tau_{xy} = -2 \operatorname{Re}[\mu_1 \mathcal{U}_1''(z_1) + \mu_2 \mathcal{U}_2''(z_2)]$$

and

$$\begin{aligned} u &= 2 \operatorname{Re}[P_1 \mathcal{U}_1'(z_1) + P_2 \mathcal{U}_2'(z_2)] \\ v &= 2 \operatorname{Re}[q_1 \mathcal{U}_1'(z_1) + q_2 \mathcal{U}_2'(z_2)] \end{aligned} \quad (78)$$

where

$$\begin{aligned} P_1 &= A_{11} \mu_1^2 + A_{12} - A_{16} \mu_1 \\ q_1 &= A_{12} \mu_1 + \frac{A_{22}}{\mu_1} - A_{26} \end{aligned}$$

Therefore solution to any specific problem is reduced to finding the \mathcal{U}_1 and \mathcal{U}_2 which satisfy the boundary conditions.

Referring again to figure 2 and equations (75), in the neighborhood of a crack tip $|z_1|$ and $|z_2|$ are small compared to

other planar dimension of problems. Consequently, the stress functions for cracks given by Lekhnitzki [83] may be reduced to the form,

$$\begin{aligned} U_1''(z_1) &= \frac{f_1(\mu_1, \mu_2, z_1)}{\sqrt{z_1}} \\ U_2''(z_2) &= \frac{f_2(\mu_1, \mu_2, z_2)}{\sqrt{z_2}} \end{aligned} \quad (79)$$

where f_1 and f_2 are well behaved in that neighborhood and some restrictions on their form are imposed by the stress free crack surface boundary conditions. Imposing these conditions, as well as those mentioned earlier and the substituting the variable

$$z = x + iy = re^{i\theta} \quad (80)$$

the crack tip stress fields are found from equations (78), (79) and (80) and can be stated in the form

$$\begin{aligned} \sigma_x &= \frac{K_{Ia}}{\sqrt{2\pi r}} \operatorname{Re} \left[\frac{\mu_1 \mu_2}{\mu_1 - \mu_2} \left\{ \frac{\mu_2}{\sqrt{\cos \theta + \mu_2 \sin \theta}} - \frac{\mu_1}{\sqrt{\cos \theta + \mu_1 \sin \theta}} \right\} \right] + \\ &\frac{K_{IIa}}{\sqrt{2\pi r}} \operatorname{Re} \left[\frac{1}{\mu_1 - \mu_2} \left\{ \frac{\mu_2^2}{\sqrt{\cos \theta + \mu_2 \sin \theta}} - \frac{\mu_1^2}{\sqrt{\cos \theta + \mu_1 \sin \theta}} \right\} \right] \end{aligned}$$

$$\begin{aligned}
\tau_y &= \frac{K_{Ia}}{\sqrt{2\pi r}} \operatorname{Re} \left[\frac{1}{\mu_1 - \mu_2} \left\{ \frac{\mu_1}{\sqrt{\cos \theta + \mu_2 \sin \theta}} - \frac{\mu_2}{\sqrt{\cos \theta + \mu_1 \sin \theta}} \right\} \right] + \\
&+ \frac{K_{IIa}}{\sqrt{2\pi r}} \operatorname{Re} \left[\frac{1}{\mu_1 - \mu_2} \left\{ \frac{1}{\sqrt{\cos \theta + \mu_2 \sin \theta}} - \frac{1}{\sqrt{\cos \theta + \mu_1 \sin \theta}} \right\} \right] \\
\tau_{xy} &= \frac{K_{Ia}}{\sqrt{2\pi r}} \operatorname{Re} \left[\frac{\mu_1 \mu_2}{\mu_1 - \mu_2} \left\{ \frac{1}{\sqrt{\cos \theta + \mu_1 \sin \theta}} - \frac{1}{\sqrt{\cos \theta + \mu_2 \sin \theta}} \right\} \right] + \\
&+ \frac{K_{IIa}}{\sqrt{2\pi r}} \operatorname{Re} \left[\frac{1}{\mu_1 - \mu_2} \left\{ \frac{\mu_1}{\sqrt{\cos \theta + \mu_1 \sin \theta}} - \frac{\mu_2}{\sqrt{\cos \theta + \mu_2 \sin \theta}} \right\} \right]
\end{aligned} \tag{81}$$

where higher order terms in r have been neglected. Reiterating, μ_1 and μ_2 are dimensionless elastic constants. Notice the striking similarity of equations (81) with equations (1) and (2). The definitions of K_{Ia} and K_{IIa} have been chosen to be identical to K_I and K_{II} for the cases of symmetrical configurations with symmetric or skew-symmetric loadings, respectively.

Consequently, it can be shown that for the general anisotropic problem of the configuration illustrated in figure 1 that:

$$K_{Ia} = \sigma \sqrt{\pi a} \tag{82}$$

$$K_{IIa} = 0$$

and for the problem in figure 2,

$$\begin{aligned} K_{IIa} &= \tau \sqrt{\pi a} \\ K_{Ia} &= 0 \end{aligned} \quad (83)$$

Moreover, for the symmetrical wedge force problem, as shown in figure 23, the stress functions are:

$$\begin{aligned} U_1'(\mathcal{J}_1) &= \frac{i P \mu_2}{2\pi(\mu_1 - \mu_2)} \log \left[\frac{\mathcal{J}_1 + \sqrt{\mathcal{J}_1^2 - a^2} - i a}{\mathcal{J}_1 + \sqrt{\mathcal{J}_1^2 - a^2} + i a} \right] \\ U_2'(\mathcal{J}_2) &= \frac{-i P \mu_2}{2\pi(\mu_1 - \mu_2)} \log \left[\frac{\mathcal{J}_2 + \sqrt{\mathcal{J}_2^2 - a^2} - i a}{\mathcal{J}_2 + \sqrt{\mathcal{J}_2^2 - a^2} + i a} \right] \\ (\mathcal{J}_k &= + a + z_k) \end{aligned} \quad (84)$$

Upon using equations (78), (79), and (80) with equations (84) and comparing results with equations (81), it is found that

$$\begin{aligned} K_{Ia} &= \frac{P}{\sqrt{\pi a}} \\ K_{IIa} &= 0 \end{aligned} \quad (85)$$

equations (85) can also be obtained from the isotropic case, equations (32) or (33), directly. It is therefore easy to add a multitude of examples by simply constructing stress

intensity factors from symmetric and skew-symmetric isotropic counterparts. Attention shall now be turned to the condition of pure shear.

(2) Pure Shear: For this case the generalized Hooke's law, equations (71), may be reduced by the definition of pure shear to:

$$\begin{aligned}\gamma_{yz} &= \frac{\partial w}{\partial y} = A_{44} \tau_{yz} + A_{45} \tau_{xz} \\ \gamma_{xz} &= \frac{\partial w}{\partial x} = A_{54} \tau_{yz} + A_{55} \tau_{xz}\end{aligned}\tag{86}$$

where $A_{54} = A_{45}$. Substituting these expressions into the equilibrium equations, the result is

$$A_{44} \frac{\partial^2 w}{\partial x^2} - 2 A_{45} \frac{\partial^2 w}{\partial x \partial y} + A_{55} \frac{\partial^2 w}{\partial y^2} = 0\tag{87}$$

which can be written

$$D_5 \cdot D_6 \cdot w = 0\tag{88}$$

where, as previously defined,

$$D_k = \frac{\partial}{\partial y} - \mu_k \frac{\partial}{\partial x}$$

Comparing equations (87) and (88) μ_5 and μ_6 are the roots of

$$A_{55} \mu^2 - 2 A_{45} \mu + A_{44} = 0 \quad (89)$$

it is observed that these roots are a conjugate pair, i.e.

$\mu_6 = \bar{\mu}_5$. Define a complex variable z_5 by

$$z_5 = x + \mu_5 y \quad (90)$$

the general solution to equation (88) may be expressed as

$$w = W_1(z_5) + W_2(\bar{z}_5) \quad (91)$$

Since w must be real, for convenience W_2 can be taken as the negative of W_1 or

$$w = 2 \operatorname{Im} [W_1(z_5)] \quad (92)$$

Referring to figure 2 for a description of the coordinates, in order to satisfy the stress free crack surface conditions W takes the form,

$$W_1 = A \sqrt{z_5} \quad (93)$$

where A is a real constant in the vicinity of the crack tip. Making use of equations (80), (86), (90), (92), and (93) the stress may be written in the form:

$$\begin{aligned}\tau_{yz} &= \frac{K_{IIIa}}{\sqrt{2\pi r}} \operatorname{Re} \left[\frac{1}{\sqrt{\cos \theta + \mu_5 \sin \theta}} \right] \\ \tau_{xz} &= \frac{K_{IIIa}}{\sqrt{2\pi r}} \operatorname{Re} \left[\frac{\mu_5}{\sqrt{\cos \theta + \mu_5 \sin \theta}} \right]\end{aligned}\quad (94)$$

where it is necessarily implied that near the crack tip

$$A = \frac{K_{IIIa} \sqrt{A_{44} A_{55} - A_{45}^2}}{\sqrt{2\pi}} \quad (95)$$

The anisotropic stress intensity factor, K_{IIIa} , is defined so that it is also identical to its isotropic counterpart, K_{III} , for all boundary value problems of pure shear. For example the configuration in figure 5 the result is

$$K_{IIIa} = K_{III} = \tau \sqrt{\pi a} \quad (96)$$

upon constructing the solution and comparing the result with equation (7).

Consequently, it has been shown that, for the general homogeneous anisotropic case the crack tip stress fields and their intensity factors, the complete analogy with the isotropic case is preserved. By judicious definition of the

anisotropic stress intensity factors, they are identical to those for the isotropic case. The resulting stress field equations (81) and (94), when superimposed* give the most general state of stress in the neighborhood of a crack tip in an anisotropic body with any configuration or loading.

Perhaps most important of all is the fact that like the isotropic case, the $1/\sqrt{r}$ singularity appears in the stress field equations (81) and (94). This fact implies that fracture size effects for homogeneous anisotropic media will be identical to the isotropic case.

However, for non-homogeneous anisotropy, such as polar orthotropy, discussed by Williams [79], singularities other than the $1/\sqrt{r}$ type may appear causing different size effects than the isotropic case.

Cracks in Linear Visco-Elastic Media

The deformation of cracks in plane viscous extension has been studied by Berg [84, 85]. He has shown that in a linear viscous sheet elliptical holes (including the

* Components of stress eliminated from the stress-strain laws should be reintroduced. They are derivable directly from the listed components in equations (81) and (94) and equations (71).

limiting cases of cracks and circles) always deform into other ellipses for the cases where additional separation is not taking place. The exclusion of separation means that adjacent points on the contour of the hole are remaining adjacent. This assumption may be somewhat restrictive, but it permits the important conclusion of ellipses deforming into ellipses, which in turn allows the use of increments of infinitesimal deformation analysis to provide a stress analysis of this class of problems.

Therefore for stationary cracks Berg has shown that the treatment by Sih [86] of stress fields near sharp crack tips for arbitrary linear viscoelasticity is in fact pertinent even though "blunting" of the crack tip takes place. Sih has shown that the crack tip stress fields are as given in equations (1), (2), and (3) where the stress intensity factors are functions of time, i.e.

$$\begin{aligned}K_I &= K_I(t) \\K_{II} &= K_{II}(t) \\K_{III} &= K_{III}(t)\end{aligned}\tag{97}$$

These stress intensity factors may be regarded as representing the time history of intensity of a crack tip stress field of constant special distribution.

Treatment of problems of moving (extending) cracks in viscoelastic media is currently unknown. However, they are obviously pertinent to formulating the condition instability of cracks in viscoelastic media where slow growth precedes sudden failure.

On the other hand the fact that equations (1), (2), and (3) have been shown to apply to any crack in a linear viscoelastic body, leads to the conclusion that slight amounts of viscous action may cause time effects but size effect will be identical to the elastic case. Consequently viscous "strain rate effects" in studies of fracture, see for example [87, 88 and 89], may be based on the usual elastic stress analysis, i.e. equations (1), (2), and (3), etc.

Some Special Cases on Non-Homogeneous Media with Cracks

The general problem of non-homogeneous media with cracks has as yet not been attacked. However, some special cases of practical interest have been treated.

The problem of two semi-infinite half planes of different material bonded (or welded) together along a line (or plane) containing a crack has received the most attention [90, 91, 92, and 93]. The applications of these analyses

include faults in laminations in rock or other materials, cracks formed at steps in the thickness of plates in extension and/or bending; stresses in glued joints and bond cracks in composite materials.

The stress fields [90, 91] for crack tips along such bond lines take the form:

$$\sigma_{ij} = \frac{K}{\sqrt{2\pi r}} f_{ij}(\epsilon, \log r) \quad (98)$$

where the terms of the type "log r" are shown [91] to be of little influence on the stress fields. Consequently, the $1/\sqrt{r}$ type of singularity is the controlling factor in the stress field. Therefore, again the dimensional character of K is preserved and fracture size effects will be identical to the homogeneous case.

However, Zak [94] observed that for a crack perpendicular to and reaching an interface between two materials, the coefficient, \mathcal{M} , of the stress singularity, $r^{-\mathcal{M}}$, will be other than 1/2. If the new material being entered by the crack has a lower modulus of elasticity then \mathcal{M} will be greater than 1/2 and vice versa. This seems to indicate a tendency to promote the entering of cracks in hard materials into softer ones due to the increased severity of the type of singularity.

Another implication here is that size effects in transmitting fracture from the harder phases of composites materials to a softer matrix will be different than the case of cracks in homogeneous materials. (More specifically the stress required for failure will depend inversely upon the size of the hard phase grains to the n^{th} power.

Inertial Effects on the Stress Field of a Moving Crack

Long before many solutions to elasto-static crack problems were available, Yoffe [95] presented the steady state solution to a crack of constant length, $2a$, moving through plate subjected to uniform tension, σ . Moreover, she noted that the extending crack tip possessed a stress field of the form,

$$\sigma_{ij} = \frac{\sigma \sqrt{\pi a}}{\sqrt{2\pi r'}} g_{ij}(\theta, C, E, \nu, \gamma) \quad (99)$$

where $\sigma \sqrt{\pi a}$ can be recognized as the stress-intensity-factor, C is the crack velocity and γ is the mass density of the material. Notice that for all values of the crack velocity the $1/\sqrt{r'}$ singularity is preserved. McClintock [96] obtained similar results for steady state problems of the mode III variety, pure shear. Both note that g_{ij} is virtually the same as the static case, equations (1), up to crack speeds, C , of over 0.4 of the shear wave velocity, C_2 , where

$$C_2 = \sqrt{\frac{E}{2(1+\nu)\gamma}} \quad (100)$$

However, at some velocity C in the neighborhood of $0.5 C_2$, the location of the maximum in θ - direction stresses changes from $\theta = 0^\circ$ to an angle of about $\theta = 60^\circ$ to the crack tip and the distribution of stresses, σ_{ij} , in general becomes quite different than the static case. The highest triaxiality of stresses near the crack tip shifts from directly ahead of the crack to about $\theta = 60^\circ$ which is most easily observed from the calculations of Baker [97]. Other authors [98, 99, 100] have reemphasized these observations, including the transient states [97].

Experimental photoelastic studies [101] confirm these results and observations of crack branching at velocities near $0.5 C_2$ add further evidence.

In addition Mott [102] and Roberts [103] studied the acceleration of a crack through dimensional considerations and obtained results tentatively in agreement with those above.

Most important in this discussion of dynamic effects is that the stress fields, equation (99), are preserved in a form nearly identical to the elastic stress up to very high velocities, i.e. $C \rightarrow 0.5 C_2$. Moreover, the $1/\sqrt{r}$ singularity appears for all velocities so that fracture size effects are virtually unchanged.

Energy Rate Analysis of Crack Extension

Griffith [1] in his original analysis of fracture and later Irwin [104] and Orowan [105] discussed the equilibrium and stability of cracks from an energy rate view point. Subsequently, Irwin [106, 4, 5] provided a more detailed study of the energy rate analysis and its relationship to the crack tip stress field approach. The details were further generalized and clarified by other authors [44, 107, 108]. The results of these works prove the equivalence of the energy rate and stress intensity factor approaches. Application to "compliance calibration" (i.e. experimental determination of energy rates) of test configurations is an additional benefit. This discussion will proceed to cover the essential features energy considerations.

An elastic body subjected to loads and containing an extending crack provides an energy rate (i.e. per unit of new crack areagenerated) \mathcal{G} , available for the crack extension process. Referring to figure 24, the available energy for an increment of crack extension, dA , is provided from work done by the force, $Pd\Delta$, and the release, $-dV$, in the total strain energy, V , stored in the body [106]. Consequently,

$$\mathcal{G} = P \frac{d\Delta}{dA} - \frac{dV}{dA} \quad (101)$$

the displacements of a linear elastic body are related to the load by

$$\Delta = \lambda P \quad (102)$$

where λ is the compliance (i.e. inverse spring constant), which depends upon the configuration including the crack size A .

The strain energy in the body is work done in loading, i.e.

$$V = \frac{P\Delta}{2} = \frac{\lambda P^2}{2} \quad (103)$$

from equations (102) and (103) and using the rule of differentiation,

$$\frac{d}{dA} = \frac{\partial}{\partial A} + \frac{dP}{dA} \cdot \frac{\partial}{\partial P} \quad (104)$$

equation (101) becomes

$$\mathcal{G} = \frac{P^2}{2} \frac{\partial \lambda}{\partial A} \quad (105)$$

terms involving dP cancel in equation (105). Therefore the available energy rate, \mathcal{G} , for infinitesimal crack extension is independent of the type of load application, e.g. fixed grips, constant forces, or intermediate cases. This result applies for an unlimited number of forces on the body [44] and for mixed types of load application [107].

Equation (105) is useful for the experimental determination of energy rates of test configurations. This is accomplished through measurement of the compliance, λ , as a function of crack size, A , in order to compute the derivative in equation (105). Though this so called "compliance calibration" method is straight forward in principal, the derivative depends on small changes in λ , which in practice require very accurate measurement techniques.

The Equivalence of Energy Rate and Stress Intensity Factor Approaches

In the previous section it was noticed that the energy rate, \dot{G} , is independent of the type of load application. Hence, for convenience in the discussion to follow the "fixed grip" situation may be employed with no loss in generality of results.

If an elastic body is loaded and the grips (load point displacements) are then fixed, the strain energy change, $\frac{dV}{dA}$, is the only contribution to, \dot{G} ; see equation (101). Under this condition the work required to close a small segment of the crack, a , as shown in figure 25, from the opened position, (a), to the closed position, (b), is identical to the change in the strain energy. The work can be computed as the crack surface tractions required to close the crack times their closing displacements times one half, (since the displacements will be

proportional to the tractions). The tractions required are the stresses on the prospective crack surface with the tip at $x = 0$ as in figure 25 (b). The displacements are the crack surface displacements of corresponding points in figure 25(a).

Therefore, as originally proposed by Irwin [4, 5, 7], the energy rate, \mathcal{G} , can be obtained from these considerations in the form

$$\mathcal{G} = \frac{dV}{dA} \Big|_{\text{fixed grips}} = \lim_{\alpha \rightarrow 0} \frac{2}{\alpha} \int_0^{\alpha} \left(\frac{\sigma_y v}{2} + \frac{\tau_{yx} u}{2} + \frac{\tau_{yz} w}{2} \right) dx \quad (106)$$

The stresses σ_y , τ_{yx} and τ_{yz} may be obtained from the crack tip stress field equations, such as equations (1), (2) and (3) with $r = x$ and $\theta = 0$. The corresponding displacements are also those of the crack tip field equations but with $r = \alpha - x$ and $\theta = \pi$.

For the isotropic case the result of these substitutions and performance of the integration in equation (106) leads to (for plane strain):

$$\mathcal{G} = \frac{1-\nu}{2G} K_I^2 + \frac{1-\nu}{2G} K_{II}^2 + \frac{1}{2G} K_{III}^2 \quad (107)$$

The terms on the right hand side of equation (107) indicate that the energy rate contribution of each mode of crack tip stress field may be considered separately. Since $E = 2(1+\nu)G$,

the separate contributions are (for plane strain):

$$\begin{aligned} \mathcal{G}_I &= \frac{(1-\nu^2)}{E} K_I^2 \\ \mathcal{G}_{II} &= \frac{(1-\nu^2)}{E} K_{II}^2 \\ \mathcal{G}_{III} &= \frac{1+\nu}{E} K_{III}^2 \end{aligned} \quad (108)$$

where

$$\mathcal{G} = \mathcal{G}_I + \mathcal{G}_{II} + \mathcal{G}_{III} \quad (109)$$

Equations (108) and (109) also may be adopted to the case of plane stress by appropriately discarding the $(1-\nu^2)$ in the first two of equations (108).

As a consequence of equations (108) and (109) the direct relationship between energy rates and stress intensity factors has been illustrated.

Equation (106) can also be used to determine the relationships between energy rates and stress intensity factors for other elastic media. For example, the relationships for anisotropic media can be obtained by using the appropriate stress fields, equations (81) and (94), and corresponding displacements in (106). Table VI provides the modified elastic coefficients for the equivalent of equations (108) and (109) for orthotropic [32] and general anisotropic [33] media.

Table VI

$$G_1 = c K_1^2$$

(Values of c given below for the case of plane strain)

<u>Mode</u>	<u>Isotropic</u> [5]	<u>Orthotropic</u> [32] ($A_{16}=A_{26}=A_{45}=0$)	<u>Anisotropic</u>
I	$\frac{(1-\nu^2)}{E}$	$\sqrt{\frac{A_{11}A_{22}}{2}} \cdot \left[\frac{A_{22}}{A_{11}} + \frac{2A_{12}+A_{66}}{2A_{11}} \right]^{1/2}$	$\frac{1}{2} \text{Im} \left[-A_{22} \frac{(\mu_1+\mu_2)}{\mu_1\mu_2} \right]$
II	$\frac{(1-\nu^2)}{E}$	$\frac{A_{11}}{2} \left[\frac{A_{22}}{A_{11}} + \frac{2A_{12}+A_{66}}{2A_{11}} \right]^{1/2}$	$\frac{1}{2} \text{Im} [A_{11}(\mu_1+\mu_2)]$
III	$\frac{(1+\nu)}{E}$	$\frac{1}{2\sqrt{A_{44}A_{55}}}$	$\frac{1}{2} \frac{\sqrt{A_{44}A_{55}-A_{45}^2}}{A_{44}A_{55}}$

However, since cracks normally do not extend in a planar fashion [57] with K_{II} and K_{III} present, or even with K_I present in generally anisotropic media, these relationships are somewhat of academic interest. It is sufficient to have shown the equivalence of the energy rate and stress intensity factor approaches, in order that the direct relationship between the Griffith theory and current theories of fracture mechanics be fully understood.

Other Equivalent Methods of Stress Analysis of Cracks and Notches

Several other methods of stress analysis of cracks and notches for incorporation into failure criteria have been proposed. The most notable in the recent literature are those developed by Neuber [10, 109], Kuhn [71, 110], and Barenblatt [23]. Identical to the elastic field approach, each of these methods uses an elastic stress analysis to determine the general character of redistribution of force transmission around cracks. In addition it is important to note that each of these analyses draws attention to a phenomena at the crack tip which is regarded as that which precipitates failure.

More specifically, these phenomena are: developing a "plastic particle" of critical size, developing the "ultimate stress" at a specific radius from the crack tip, and developing stresses approaching the "cohesive bond forces" ahead of a crack, respectively. Now, since each of these phenomena occur imbedded within the elastic crack tip stress field, their occurrence will always correspond to having that stress field reach a critical value. As a consequence these and any other methods which draw attention to specific critical phenomena at a crack tip, which proceed to use an essentially elastic stress analysis, will lead to a failure theory equivalent to the current fracture mechanics concept of critical values of stress-intensity-factors.

Even though these alternative methods may be regarded as just as true, correct and, useful in a practical sense, the attention that each draws to a specific phenomena within the crack tip stress field embodies an assumption which is unnecessarily restrictive in formulating a failure criteria. The strength and generality of "fracture mechanics" as based on the stress field approach is in part due to the absence of such an assumption.

On the other hand this does not mean that the phenomena which do in fact occur within the stress fields near crack tips should be disregarded. Attention to the details of the processes by which materials resist cracking will undoubtedly lead to development of superior materials. Each of the alternative "theories of fracture" mentioned above (and others) does in fact draw attention to a phenomena which may be a key feature in the fracture process. Therefore their high worth in conjunction with and complimentary to the methods of "fracture mechanics" is clear.

Limitations of the Crack Tip Stress Field Analyses

In this paper results of linear elastic stress analyses of cracked bodies have been presented for a typical variety of problems which have already been treated. The determination stress-intensity-factors for any particular problem can with time be accomplished. Therefore the elastic stress analysis is not in itself a real limitation fracture mechanics.

However, the accomplishment of a stress analysis does represent a delay in the application of fracture mechanics to configurations with cracks which have not yet been treated. Moreover, the accuracy of known solutions for stress-intensity-factors represents a temporary limitation on the accuracy of immediate applications. Usually, this limitation is far less severe than others, such as variability of materials, in practical applications.

Consequently, the elastic stress analyses itself may be regarded as "exact" and the real limitations of fracture mechanics come only in its application to situations where non-linearity of material behavior at the crack tip (or elsewhere) disrupts the gross features of the stress distribution.

A certain amount of nonlinear behavior such as plasticity can be tolerated within the crack tip stress field without grossly effecting the field outside the nonlinear region.

Moreover, the disturbances, if embedded within identical fields, will themselves be identical and hence self-compensating in comparisons of fracture strengths. Therefore it is important to resolve the relative sizes of zones of non-linearity which can be tolerated within the crack tip stress fields. This size is of course related to the relative size in which the field equations, such as equations (1), apply.

For the configuration shown in figure 3, the approximate stress, σ_y , ahead of the crack, obtained by substituting equation (4) into (1) and setting $\theta = 0$, is:

$$\sigma_y \text{ approx.} = \frac{\sigma\sqrt{a}}{\sqrt{2r}} \quad (109)$$

The exact stress can be most easily determined by the Westergaard stress function technique, see Appendix I, and is:

$$\sigma_y \text{ exact} = \frac{\sigma(a+r)}{\sqrt{2ar+r^2}} \quad (110)$$

where in equations (109) and (110), r is the distance ahead of the crack tip along the crack line.

Now, taking the ratio of the exact to the approximate stresses gives:

$$\frac{\sigma_y \text{ approx}}{\sigma_y \text{ exact}} = \frac{\sqrt{1+2\frac{r}{a}}}{(1+\frac{r}{a})} \quad (111)$$

In a similar fashion this ratio may also be computed for the configuration shown in Figure 23 and is:

$$\frac{\sigma_y \text{ approx}}{\sigma_y \text{ exact}} = \left(1 + \frac{r}{a}\right) \sqrt{1 + \frac{r}{2a}} \quad (112)$$

The types of loading in these two configurations, Figure 3 and 23, are opposite extremes, yet equations (111) and (112) show similar deviations of the approximate stresses from the exact at like values of r/a . Therefore if the relative tolerable size (compared to crack size, a) of zone of nonlinearity can be established for one configuration it is bound to be applicable to others.

Recent experimental evidence [75] indicates the validity of the elastic stress field approach up to stress levels σ of 0.8 of the yield strength, $\sigma_{y.p.}$, for the configuration shown in Figure 3. For this configuration the width, w , of the zone of plasticity is predicted to be [78]:

$$w = \frac{1}{2} \left(\frac{\sigma}{\sigma_{y.p.}}\right)^2 a \quad (113)$$

Substituting the upper limit of stress, $\sigma = 0.8 \sigma_{y.p.}$, mentioned above, the relative size w/a or r/a for reasonable accuracy is about 0.3 from equation (113). For this value of r/a , equation (111) predicts a deviation of actual stresses from

the field equations of about 20%. Thus the zone of nonlinearity at a crack tip may be fairly sizable, i.e. of the order of 0.3 of the crack length (and other planar dimensions such as net section width), without grossly disturbing the usefulness of the elastic stress field approach. However, a more extensive evaluation of this limitation should be the subject of further research.

In addition to non-linearity in the region of the crack tip consideration of other conditions, such as anisotropic and viscous effects, having cracks in the bond line between dissimilar materials, thermal stresses, couple stresses, inertial effects of moving cracks, as well as considering all three modes of crack tip stress fields, has led to positive results. The conclusion is that the current techniques of "fracture mechanics" may be extended to all of these areas, since similar types of crack tip stress fields exist for them and the stress-intensity-factor methods of assessing failure should apply equally well. At any rate this conclusion should give full confidence that slight amounts of these effects do not invalidate the useful application of the concepts of fracture mechanics.

As a consequence of the above remarks, it is observed that the only real limitation of elastic stress analysis of commences with the advent of sizable zones of non-linearity

i.e. plasticity, at the crack tip. The current hope for extension of the applicability of "fracture mechanics" to such situations lies in developing a full analysis based "the theory of plasticity". This topic is a subject left for other discussions.

Acknowledgement

The authors gratefully acknowledge the support of this work under the NASA grant Nsg 410 to the Lehigh University Institute of Research. Portions of the analysis based on previous work were supported under grants from the National Science Foundation, G24145, and the Boeing Company.

The many suggestions and data provided by Dr. W.F. Brown, Dr. O.L. Bowie and Dr. G.R. Irwin were most helpful in preparation to this paper. Appreciation is also expressed for aid in collecting information for Appendix II given by Mr. M. Kassir of the Department of Mechanics of Lehigh University.

References:

- 1) Griffith, A.A. "The Phenomena of Rupture and Flow in Solids" the Philosophical Transactions of the Royal Society of London, Vol. 221, 1920.
- 2) Inglis, C.E. "Stresses in a Plate Due to the Presence of Cracks and Sharp Corners" Proceedings of the Institute of Naval Architects, Vol. 60, 1913.
- 3) Sneddon, I.N. "The Distribution of Stress in the Neighborhood of a Crack in an Elastic Solid", Proceedings of the Royal Society of London, Vol. A-187, 1946.
- 4) Irwin, G.R. "Analysis of Stresses and Strains near the End of a Crack Traversing a Plate", the Journal of Applied Mechanics, A.S.M.E., June 1957.
- 5) Irwin, G.R. "Fracture" Handbuch der Physik, Vol. VI, Springer, 1958.
- 6) Williams, M.L. "On the Stress Distribution at the Base of a Stationary Crack", Journal of Applied Mechanics, A.S.M.E., March 1957.
- 7) Irwin, G.R. "Fracture Mechanics", Structural Mechanics, Pergamon Press, 1960.
- 8) Westergaard, H.M. "Bearing Pressures and Cracks", Journal of Applied Mechanics, A.S.M.E., June 1939.
- 9) Paris, P.C. "Stress-Intensity-Factors by Dimensional Analysis", Lehigh University, Institute of Research Report, 1961.
- 10) Neuber, H. "Kerbspannungslehre", Springer, 1937 and 1958 (English translation available from Edwards Bros., Ann Arbor, Mich.)
- 11) Peterson, R.E. Stress Concentration Design Factors, John Wiley & Sons, 1953.
- 12) Savin, G. Stress Concentration Around Holes, Pergamon Press, 1961.
- 13) Isida, M. "The Effect of Longitudinal Stiffeners in a Cracked Plate under Tension", Proc. of the 4th U.S. Cong. of Appl. Mech., 1962.

- 14) Kobayashi, A.S. and R.G. Forman "On the Axial Rigidity of a Perforated Strip and the Strain Energy Release Rate in a Centrally Notched Strip Subjected to Uniaxial Tension" A.S.M.E. preprint No. 63-WA-29 (to be published in The Journal of Basic Engineering).
- 15) Kobayashi, A.S.; R.B. Cherepy, and W.C. Kinsel "A Numerical Procedure for Estimating the Stress Intensity Factor of a Crack in a Finite Plate" A.S.M.E., preprint No. 63-WA-24 (to be published in The Journal of Basic Engineering).
- 16) Bowie, O.L. "Rectangular Tensile Sheet with Symmetric Edge Cracks" A.S.M.E. paper No. 64-APM-3 (to be published in The Journal of Applied Mechanics).
See also: Bowie, O.L. and Neal, D.M. "Single Edge Cracks in Rectangular Tensile Sheet" Tech. rep. AMRA TR 64-13, Watertown Arsenal, May 1964.
- 17) Muskhelishvili, N.I. Some Basic Problems of Mathematical Theory of Elasticity, 1933, English translation, P. Noordhoff and Company, 1953.
- 18) Sih, G., P. Paris and F. Erdogan "Crack Tip Stress Intensity Factors for Plane Extension and Plate Bending Problems", Journal of Applied Mechanics, A.S.M.E., June 1962.
- 19) Sokolnikoff, I.S. Mathematical Theory of Elasticity, McGraw-Hill Book Company, 1956.
- 20) Sanders, J.L., Jr. "On the Griffith-Irwin Fracture Theory", Journal of Applied Mechanics, A.S.M.E., 1960.
- 21) Erdogan, F.E. "On the Stress Distribution in Plates with Colinear Cuts under Arbitrary Loads", proceedings of the 4th U.S. National Congress of Applied Mechanics, 1962.
- 22) Sih, G. "Application of Muskhelishvili's Method to Fracture Mechanics", transactions of The Chinese Association for Advanced Studies, November 1962.
- 23) Barenblatt, G.I. "Mathematical Theory of Equilibrium Cracks in Brittle Fracture", Advances in Applied Mechanics, VII, Academic Press, 1962.
- 24) Sih, G. "On Crack Tip Stress-Intensity-Factors for Cylindrical Bars under Torsion", The Journal of The Aerospace Sciences, October 1962.

- 25) Sih, G. "The Flexural Stress Distribution near a Sharp Crack", Journal of A.I.A.A., February 1963.
- 26) Sih, G. "Strength of Stress Singularities at Crack Tips for Flexural and Torsional Problems", Journal of Applied Mechanics, A.S.M.E., September 1963.
- 27) Sadowsky, M.A. and Sternberg, E.G. "Stress Concentration Around a Triaxial Ellipsoidal Cavity", Journal of Applied Mechanics, Trans. of A.S.M.E., June 1949.
- 28) Green, A.E. and I.N. Sneddon "The Stress Distribution in the Neighborhood of a Flat Elliptical Crack in an Elastic Solid", Proceedings of The Cambridge Philosophical Society, Vol. 46, 1950.
- 29) Irwin, G.R. "The Crack Extension Force for a Part through Crack in a Plate", Journal of Applied Mechanics, A.S.M.E., December 1962.
- 30) Wigglesworth, L.A. "Stress Distribution in a Notched Plate", Mathematika, Vol. 4, 1957.
- 31) Irwin, G.R. "The Crack Extension Force for a Crack at a Free Surface Boundary", N.R.L. Report No. 5120, 1958.
- 32) Irwin, G.R. "Analytical Aspects of Crack Stress Field Problems", Univ. of Illinois, T. & A.M. Report No. 213, March 1962.
- 33) Sih, G., - unpublished results
- 34) Isida, M. "On the Tension of a Strip with a Central Elliptical Hole", Trans. Japan Soc. of Mech. Engr., Vol. 21, No. 107, 1955.
- 35) Isida, M. "On the In-Plane Bending of a Strip with a Central Elliptical Hole", Trans. of Japan Soc. of Mech. Engrs., Vol. 22, No. 123, 1956.
- 36) Isida, M. "On the Tension of a Semi-Infinite Plate with an Elliptical Hole", Trans. of Japan Soc. of Mech. Engrs., Vol. 22, No. 123, 1956.
- 37) Bueckner, H.F. - Internal Reports of the General Electric Company, Schenectady, N. Y.

- 38) Bueckner, H.F. - "Some Stress Singularities and their Computation by Means of Integral Equations", Boundary Value Problems in Differential Equations (R.E. Langer Edit.), University of Wisconsin, 1960.
- 39) Winne, D.H. and B.M. Wundt "Application of the Griffith-Irwin Theory of Crack Propagation to Bursting Behavior of Disks", Transactions of A.S.M.E., Vol. 80, No. 8, November 1958.
- 40) Bowie, O.L. "Analysis of an Infinite Plate Containing Radial Cracks Originating from the Boundary of an Internal Circular Hole", Journal of Mathematics and Physics, Vol. 35, No. 1, 1956.
- 41) Gross, B.; J.E. Scrawley and W.F. Brown, Jr. "Stress Intensity Factors for a Single Edge Notched Tension Specimen by Boundary Collocation of a Stress Function" N.A.S.A., Lewis Research Center, unpublished report.
- 42) Romualdi, J.P.; J.T. Frasier and G.R. Irwin "Crack Extension Force near a Riveted Stringer", N.R.L. Report No. 4956, May 1957.
- 43) Romualdi, J.P. and P.H. Sanders "Fracture Arrest by Riveted Stiffeners", Proc. of the 4th Midwest Conference on Solid Mechanics, Univ. of Texas Press, 1959/1960.
- 44) Paris, P.C. "The Mechanics of Fracture Propagation and Solutions to Fracture Arrestor Problems", Boeing Document No. D2-2195, 1957.
- 45) Paris, P.C. "A Short Course in Fracture Mechanics", University of Washington, 1960.
- 46) Sanders, J.L., Jr. "Effect of a Stringer on the Stress Concentration Factor due to a Crack in a Thin Sheet", N.A.S.A., Tech. Rep. R-13, 1959.
- 47) Isida, M. "Stress Concentration due to a Central Transverse Crack in a Strip Reinforced on Either Side", Journ. of Japan Society of Aero-Space Sciences, Vol. 10, No. 100, 1962.
- 48) Greif, R. and J.L. Sanders, Jr. "The Effect of a Stringer on the Stress in a Cracked Sheet", Harvard University, June 1963 (to be published in the Journal of Applied Mechanics).
- 49) Sanders, J.L., Jr. - Private Communication

- 50) Terry, T. "Analysis of a Reinforced Infinite Plate Containing a Single Crack", Ph.D. dissertation, Lehigh University, September 1963.
- 51) Sih, G. "On the Singular Character of Thermal-Stresses Near a Crack Tip", Journal of Applied Mechanics, A.S.M.E., Vol. 29, 1962.
- 52) Florence, A.L. and J.N. Goodier "Thermal stress due to Disturbance of Uniform Heat Flow by an Ovaloid Hole", Journal of Applied Mechanics, A.S.M.E., Vol. 27, 1960.
- 53) Williams, M.L. "Surface Stress Singularities Resulting from Various Boundary Conditions in Angular Corners of Plates under Bending", Proc. of the First U.S. Nat. Congress of Appl. Mech., June 1951.
- 54) Williams, M.L. and R.H. Owens "Stress Singularities in Angular Corners of Plates having Linear Flexural Rigidities for Various Boundary Conditions", Proc. of the Second U.S. Nat. Congress of Appl. Mech., June 1954.
- 55) Williams, M.L. "The Bending Stress Distribution at the Base of a Stationary Crack", Journ. of Appl. Mech., A.S.M.E., March 1961.
- 56) Erdogan, F., O. Tuncel and P. Paris "An Experimental Investigation of the Crack Tip Stress Intensity Factors in Plates under Cylindrical Bending", Journ. of Basic Eng., A.S.M.E., March 1963.
- 57) Erdogan, F. and G. Sih "On Crack Extension in Plates under Plane Loading and Transverse Shear", The Journ. of Basic Engin., A.S.M.E., Dec. 1963.
- 58) Knowles, J.K. and N.-M. Wang "On the Bending of an Elastic Plate Containing a Crack", Galcit, SM 60-11, July 1960.
- 59) Reissner, E. "The Effect of Transverse Shear Deformation on the Bending of Elastic Plates", Journ. of Applied Mech., A.S.M.E., Vol. 12, 1945.
- 60) Williams, M.L. (published discussion of reference 56), (see also reference 80).
- 61) Roberts, R. - unpublished test results to be incorporated into a Ph.D. dissertation, Lehigh University.

- 62) Sih, G. and D. Setzer (discussion of reference 63),
The Journal of Applied Mechanics, A.S.M.E., June 1964.
- 63) Folias, E.S. and M.L. Williams "The Bending Stress in a
Cracked Plate on an Elastic Foundation", The Journal of
Applied Mechanics, A.S.M.E., June 1963.
- 64) Folias, E.S. - Ph.D. dissertation at Calif. Inst. of Tech.,
1963.
- 65) Ang, D.D., E.S. Folias and M.L. Williams "The Effect of
Initial Spherical Curvature on the Stresses near a Crack
Point", Galcit report, SM 62-4, May 1962.
- 66) Reissner, E. "Stress and Displacements of Shallow
Spherical Shells", Journ. of Math. and Physics, Vol. 25,
1946.
- 67) Sechler, E.E. and M.L. Williams "The Critical Crack Length
in Pressurized Cylinders", Galcit 96, final report,
Sept. 1959.
- 68) Williams, M.L. "Some Observations regarding the Stress
Field near the Point of a Crack", Proceedings of the Crack
Propagation Conference, (Cranfield, England), Sept. 1961.
- 69) Bluhm, J.I. and Mardirosian, M.M. "Fracture Arrest
Capabilities of Annularly Reinforced Cylindrical Pressure
Vessels", Experimental Mechanics, Vol. 3, Nos. 3 and 12,
March and December 1963.
- 70) Peters, R.W. and Kuhn, P. "Bursting Strength of
Unstiffened Pressure Cylinders with Slits", N.A.S.A.,
TN 3993, April 1956.
- 71) Kuhn, P. "The Prediction of Notch and Crack Strength under
Static and Fatigue Loading", presented at the SAE-ASME
Meeting, New York, April 1964.
- 72) Cosserat, Z. and F. "Théorie des Corps Déformables",
A. Hermann et Fils, Paris, 1909.
- 73) Mindlin, R.D. "Influence of Couple Stresses on Stress
Concentrations", Experimental Mechanics, Vol. 3, 1963.
- 74) Setzer, D. "An Elasto-Static Couple Stress Problem:
Extension of a Elastic Body containing a Finite Crack",
Ph.D. dissertation, Lehigh University, Dec. 1963.

- 75) Anon, "Screening Tests for High-Strength Alloys using Sharply Notched Cylindrical Specimens", 4th report of Special A.S.T.M. Committee, Materials Research and Standards, Vol. 2, No. 3, March 1962, (see also other reports Jan. 1960, Feb. 1960, May 1961, Nov. 1961 and March 1964).
- 76) Sneddon, I.N. "Crack Problems in Mathematical Theory of Elasticity", North Carolina State College, Report No. ERD-126/1, May 1961.
- 77) Bueckner, H. - Private Communication
- 78) Irwin, G.R. and McClintock, F.A. "Plasticity Modifications to Crack Stress Analysis", Proceedings of the A.S.T.M. Symposium on Fracture Testing, June 1964.
- 79) Chapkis, R.L. and M.L. Williams "Stress Singularities for a Sharp-Notched Polarly Orthotropic Plate", Proceedings of the Third U.S. Congress of Applied Mechanics, 1958.
- 80) Ang, D.D. and M.L. Williams "Combined Stresses in an Orthotropic Plate having a finite Crack", Journal of Applied Mechanics, A.S.M.E., Sept. 1961.
- 81) Willmore, T.J. "The Distribution of Stress in the Neighborhood of a Crack", Quarterly Journal of Mechanics and Applied Mathematics, Vol. II, Part I, 1949.
- 82) Sih, G.C. and P.C. Paris "The Stress Distribution and Intensity Factors for a Crack Tip in an Anisotropic Plate Subjected to Extension", Lehigh University, Institute of Research Report, October 1961.
- 83) Lekhnitzki, S.G. Anisotropic Plates, 1947, translated by E. Stowell for A.I.S.I., New York, 1956. (See alternatively a newer translation available through Holden-Day Book Co., San Francisco).
- 84) Berg, C.A. "The Influence of Viscous Deformation on Brittle Fracture", D.Sc. dissertation at M.I.T., June 1962.
- 85) Berg, C.A. "The Motion of Cracks in Plane Viscous Deformation", Proceedings of the 4th U.S. Nat. Congress of Applied Mechanics, 1962.

- 86) Sih, G.C. "Viscoelastic Stress Distribution Near the End of a Stationary Crack", Lehigh University, Institute of Research Report, July 1962.
- 87) Krafft, J. and G.R. Irwin "Crack Velocity Considerations", Proceedings of the A.S.T.M. Symposium on Fracture Testing, June 1964.
- 88) Krafft, J. and A.M. Sullivan "Effects of Speed and Temperature upon Crack Toughness and Yield Strength in Mild Steel", A.S.M. (Trans. Quart.), Vol. 56, March 1963.
- 89) Irwin, G.R. "Crack Toughness Testing of Strain Rate Sensitive Materials" (to be published in The Journal of Basic Engineering, 1964).
- 90) Williams, M.L. "The Stresses Around a Fault or Crack in Dissimilar Media", Bul. of Seismological Soc. of Amer., Vol. 49, 1959.
- 91) Erdogan, E. "Stress Distribution in a Non-Homogeneous Elastic Plane with Cracks", Journ. of Appl. Mech., A.S.M.E., Vol. 30, June 1963.
- 92) Sih, G. and J. Rice "The Bending of Plates of Dissimilar Materials with Cracks" (to be published in The Journal of Applied Mechanics, 1964).
See also: Rice, J. and Sih, G. "Plane Problems of Cracks in Dissimilar Media", Lehigh University, Institute of Research Report, April 1964 (submitted to The Journal of Applied Mechanics for publication).
- 93) Erdogan, F. and L.Y. Bahar "On the Stress Distribution in Bonded Dissimilar Materials with a Circular Cavity" (to be published in The Journal of Applied Mechanics, 1964-65).
- 94) Zak, A.R. and M.L. Williams "Crack Point Stress Singularities at a Bimaterial Interface", G.A.L. C.I.T. Report SM 62-1, January 1962.
- 95) Yoffe, E. "The Moving Griffith Crack", Philosophical Magazine, Ser. 7, Vol. 42, 1951.
- 96) McClintock, F. and P. Sukhatme "Traveling Cracks in Elastic Materials under Longitudinal Shear", Journal of Mech. and Physics of Solids, Vol. 8, 1960.

- 97) Baker, B.R. "Dynamic Stresses Created by a Moving Crack", Journal of Applied Mechanics, A.S.M.E., Vol. 29, 1962.
- 98) Craggs, J.W. "On the Propagation of a Crack in an Elastic-Brittle Material", Journal of Mech. and Physics of Solids, Vol. 8, 1960.
- 99) Ang, D.D. "Some Radiation Problems in Elastodynamics", Ph.D. dissertation, C.I.T., 1958.
- 100) Cotterell, B. "On the Nature of Moving Cracks" (to be published in The Journal of Applied Mechanics, 1964), A.S.M.E., Paper No. 63-WA-181.
- 101) Wells, A.A. and D. Post "The Dynamic Stress Distribution Surrounding a Running Crack - a Photoelastic Analysis", N.R.L. Report No. 4935, April 1957.
- 102) Mott, N.F. "Fracture of Metals: Theoretical Considerations", Engineering, Vol. 165, 1948.
- 103) Roberts, D.K. and A.A. Wells "The Velocity of Brittle Fracture", Engineering, Vol. 178, 1954.
- 104) Irwin, G.R. and Kies, J. "Fracturing and Fracture Dynamics", The Welding Journal Research Supplement, February, 1952. (and earlier work referenced therein).
- 105) Orowan, E. "Fundamentals of Brittle Behavior of Metals", Fatigue and Fracture of Metals, John Wiley & Sons, 1952 (and earlier work referenced therein).
- 106) Irwin, G.R. "A Critical Energy Rate Analysis of Fracture Strength", The Welding Journal Research Supplement, April 1954.
- 107) Bueckner, H.F. "The Propagation of Cracks and Energy of Elastic Deformation", Transactions of A.S.M.E., August 1958.
- 108) Sanders, J.L. "On the Griffith-Irwin Fracture Theory", Journal of Applied Mechanics, Vol. 27, Trans. A.S.M.E., Ser. E, Vol. 82, 1960.
- 109) Neuber, H. see: Irwin, G.R. "Fracture Mechanics" Structural Mechanics, Pergamon Press, 1960.
- 110) Kuhn, P. and I.E. Figge "Unified Notch-Strength Analysis for Wrought Aluminum Alloys", N.A.S.A., T.N. D-1259, 1962.

Table of Notation

A	Crack surface area
a	Half crack length of internal crack or crack depth of surface crack
A_{ij}	Elastic compliance coefficients for Hooke's law of plane problems of anisotropic media
a_{ij}	Elastic compliance coefficients for the general Hooke's law of anisotropic media
b	Half width of a strip
C_1, C_2	Constants
C	Crack velocity
D_k	Complex differential operators ($k=1, \dots, 6$)
D	Round bar diameter
d	notch diameter
E	Modulus of elasticity
F	$= P-iQ$, force with complex representation (per unit thickness)
G	Shear modulus of elasticity Energy rate available for crack extention
$\mathcal{G}_I, \mathcal{G}_{II}, \mathcal{G}_{III}$	Energy rates associate with each mode of cracking
h	depth of a beam or plate
i	$\sqrt{-1}$
$K = K_I - iK_{II}$	Stress intensity factor with complex representation
K_I, K_{II}, K_{III}	Stress intensity factors for each mode (subscript a indicates anisotropic type)
K_1, K_2, K_3, K_4	Stress intensity at various points on a crack countour

K_B, K_S	Plate and shell bending and shearing stress intensity factors
L	Half length of a strip
l	A couple stress elastic constant
M	Applied bending moment (per unit thickness)
P	Force (per unit thickness)
p	Crack tip radius
P_1, q_1	Anisotropic elastic constants
R	Radius of a curved crack
r	Radial coordinate from a crack tip
T	Temperature
t	Plate thickness (or time)
U, U_1, U_2	Stress functions for anisotropic media
u, v, w	Displacement components
V	Strain energy
Z, Z_I, Z_{II}, Z_{III}	Westergard stress functions
Z, Z, Z, Z'	Successive derivatives of a Westergaard stress function
z, z	complex variables
z_1, z_2, z_3	modified complex variables for anisotropic analysis
α	An angle (or closing segment of a crack)
β	An angle
γ	Mass density
$\gamma_{xy}, \gamma_{yz}, \gamma_{xz}$	Shear strain components
Δ	Displacement

∇	Gradient $\left(\frac{\partial}{\partial x} + \frac{\partial}{\partial y}\right)$
∇^2, ∇^4	Harmonic and biharmonic operators
ϵ	The bielastic constant of joined half-planes
$\epsilon_x, \epsilon_y, \epsilon_z$	Normal strain components
z	A complex variable (origin at the crack tip)
ζ_1, ζ_2	Modified complex variables for anisotropic media (origin at the crack tip)
η	Complex variable in the mapped plane
Θ	Angular coordinate measured from the crack plane
κ	An elastic constant for plane stress or strain
λ	Compliance of a linear-elastic body
μ, μ_k	Elastic constants for anisotropic media ($k=1, \dots, 6$)
ν	Poisson's ratio
σ, τ	Normal and shear stress (applied at infinity)
σ_0	Maximum stress at a notch
σ_{net}	Net section stress (average)
$\sigma_{ij} = \sigma_x, \sigma_y, \sigma_z,$	Rectangular components of stress
$\tau_{xy}, \tau_{yz}, \tau_{xz}$	
$\sigma_r, \sigma_\theta, \tau_{r\theta}$	Polar components of stress
ϕ	Airy's stress function
ϕ	A complex stress function for plane stress or strain
ϕ_0	An elliptic integral
ϕ_B	A complex stress function for plate bending
χ	A complex stress function for plane stress or strain

ψ_i Harmonic functions
F(), g(), A function of
h(), k()
Re, Im Real and imaginary parts of complex functions

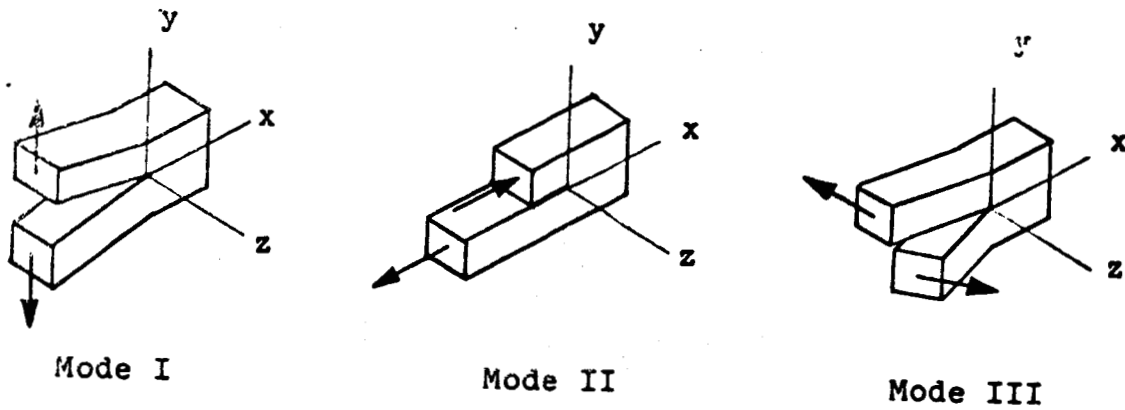


Figure 1 - The Basic Modes of Crack Surface Displacements

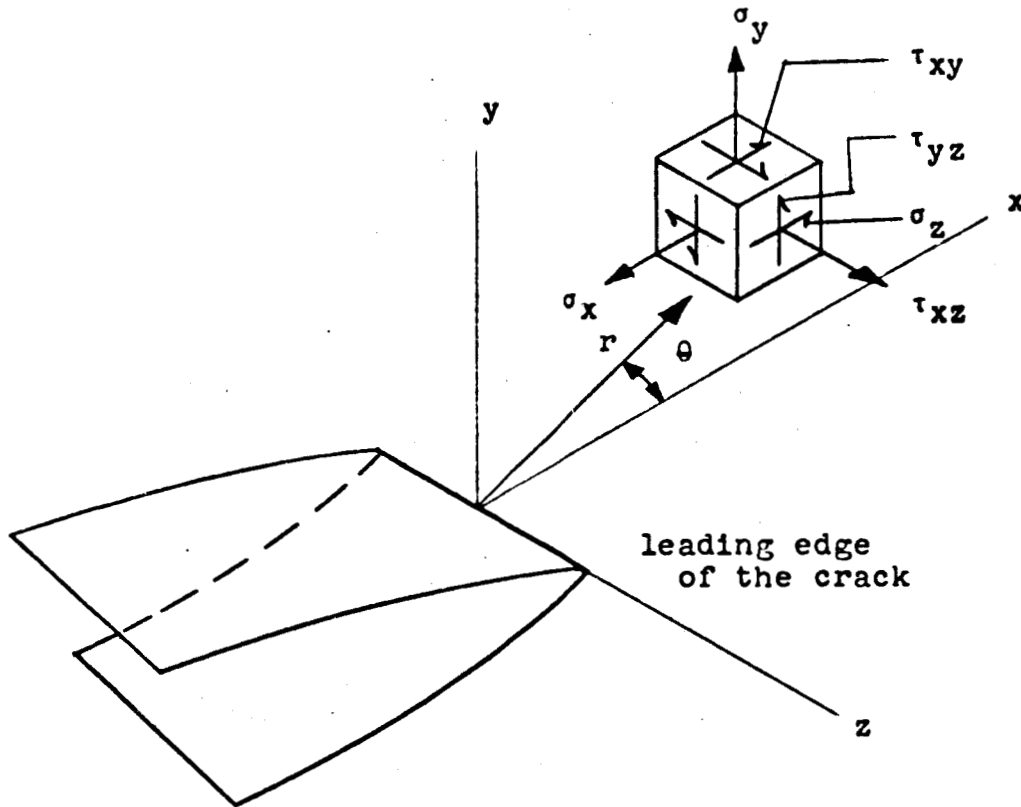


Figure 2 - Coordinates Measured from the Leading Edge of a Crack and the Stress Components in the Crack Tip Stress Field

Figure 3 - An Infinite Cracked Sheet
with Uniform Normal Stress
at Infinity

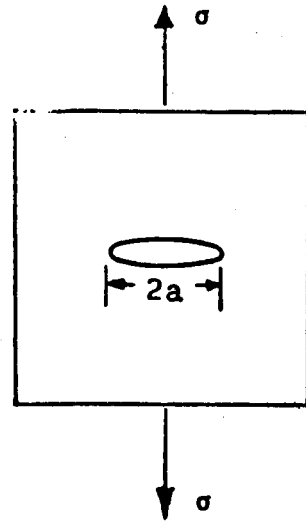


Figure 4 - An Infinite Cracked Sheet
with Uniform In-Plane Shear
at Infinity

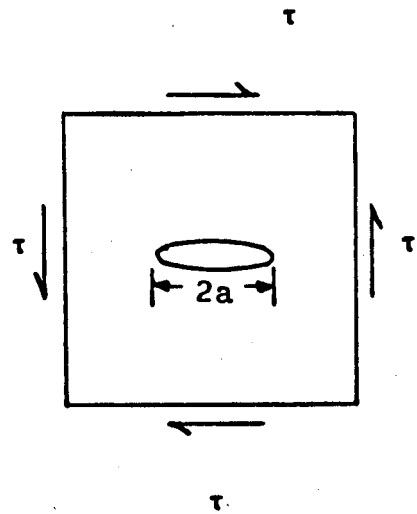
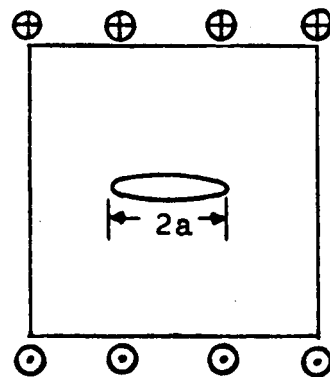


Figure 5 - An Infinite Body with a
"Tunnel Crack" subjected to
Out-of-plane Shear at Infinity



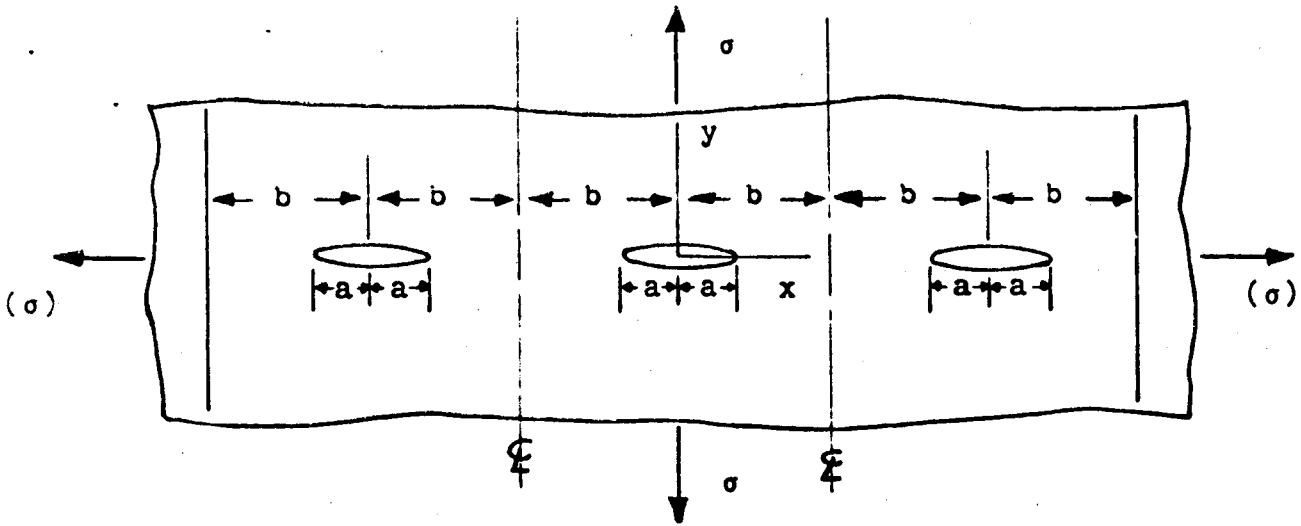


Figure 6 - A Periodic Array of Cracks along a Line in a Sheet with Uniform Stress at Infinity

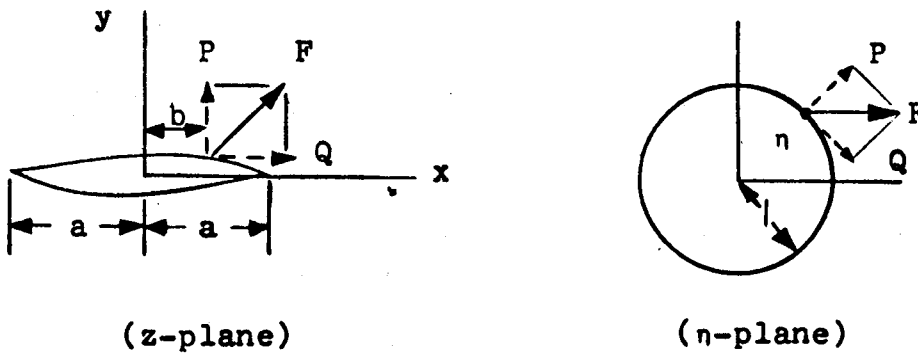


Figure 7 - A Concentrated Force (per Unit Thickness) on the Surface of a Crack in an Infinite Sheet

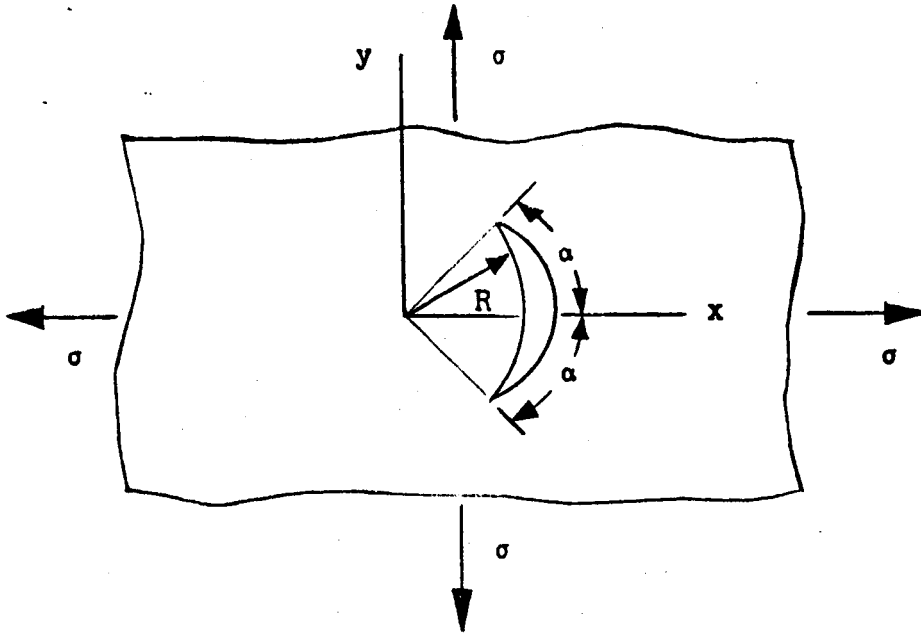


Figure 8 - A Curved Crack in an Infinite Sheet Subjected to Uniform Biaxial Tension

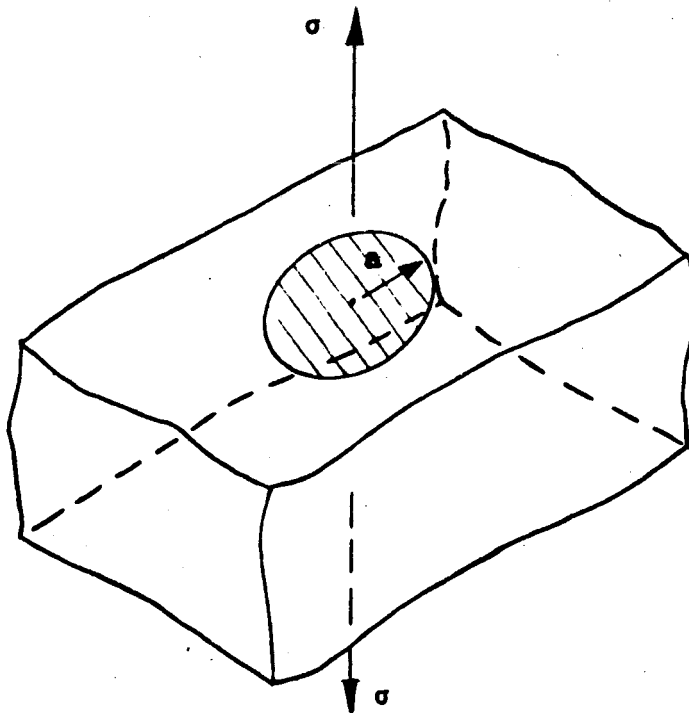


Figure 9 - A "Penny-Shaped" (Circular Disk) Crack in an Infinite Body Subjected to Uniform Tension

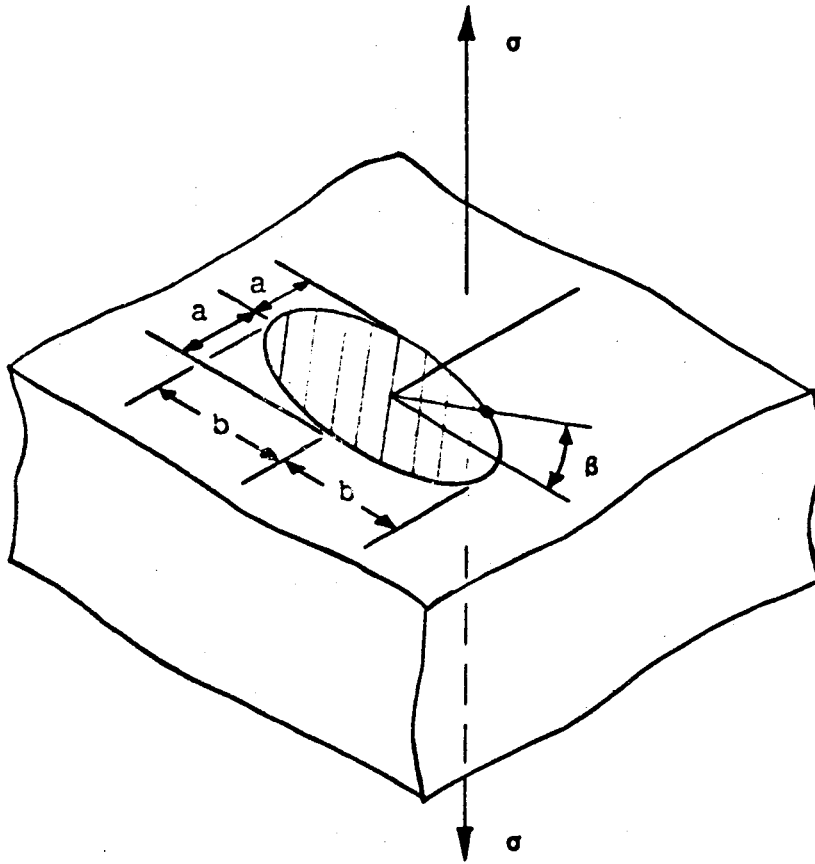


Figure 10 - An Elliptical Crack in an Infinite Body Subjected to Uniform Tension

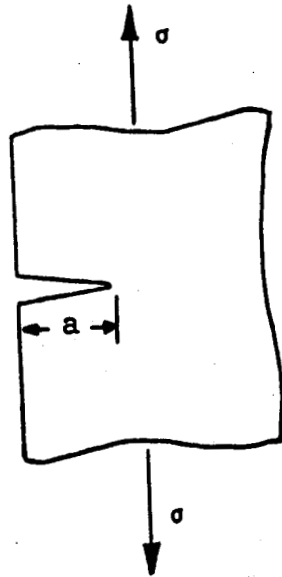


Figure 11 - An Edge Crack in a Semi-Infinite Sheet Subjected to Tension

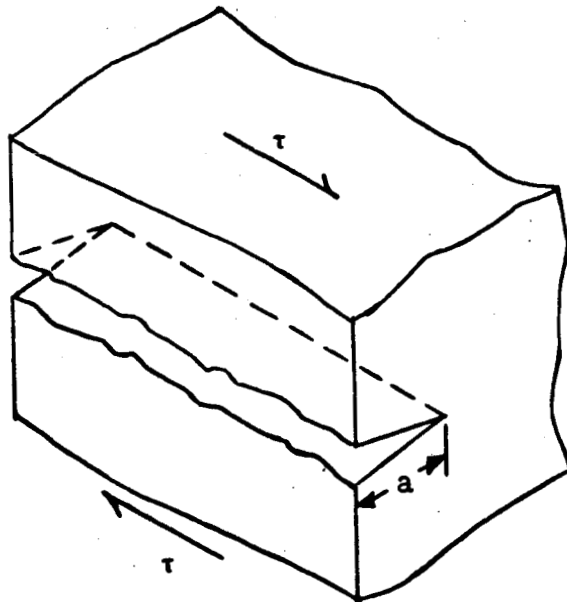


Figure 12 - An Edge Crack in a Semi-Infinite Body Subjected to Shear

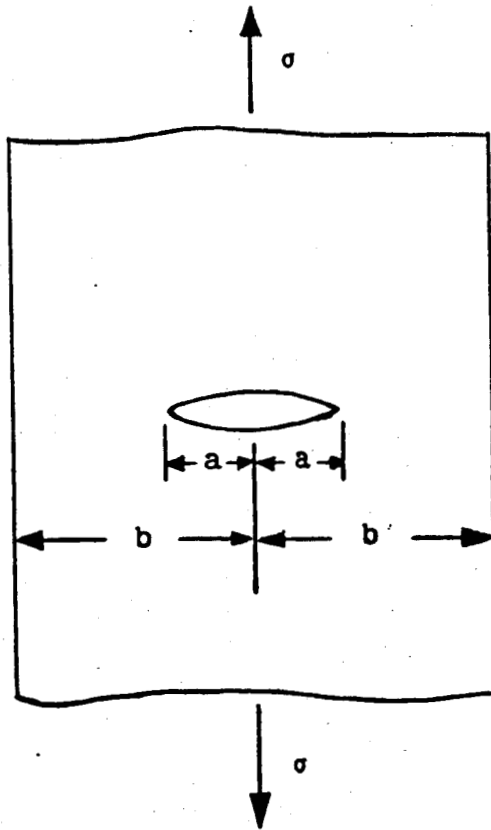


Figure 13 - A Central Crack in a Strip Subjected to Tension

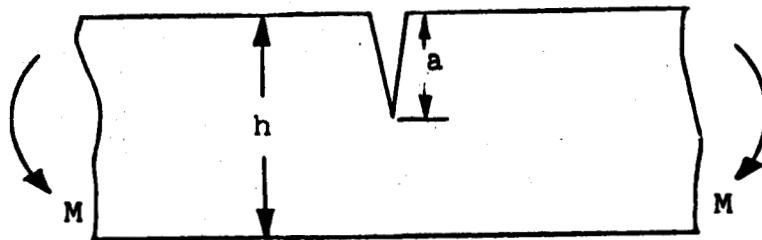


Figure 14 - An Edge Crack in a Strip Subjected to in Plane Bending

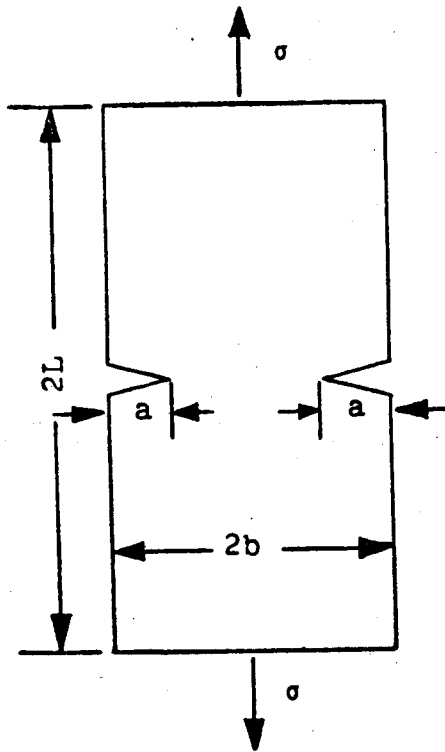


Figure 15 - Double Symmetric Edge Cracks in Strip of Finite Length Subjected to Tension

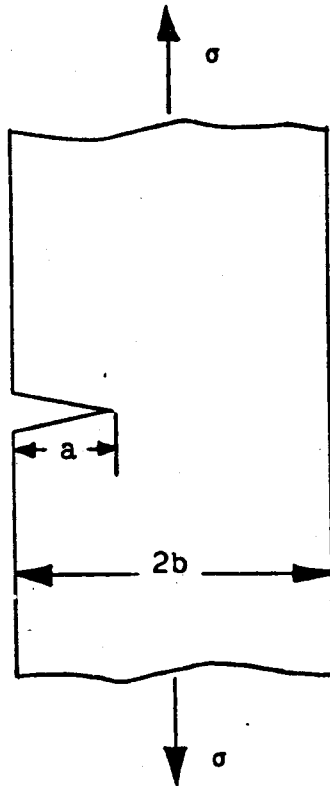


Figure 16 - A Single Edge Cracked Strip Subjected to Tension

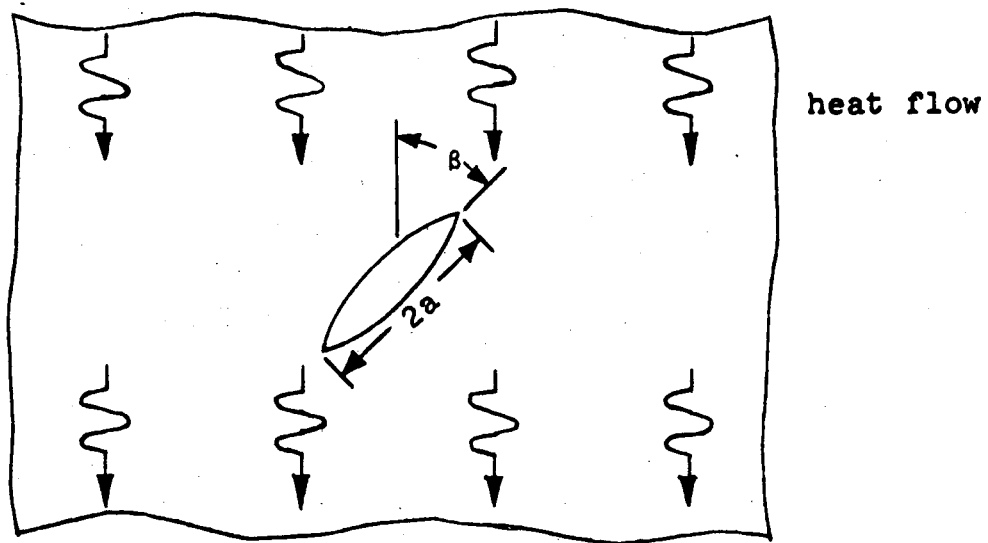


Figure 17 - An Insulated Crack
Disturbing Uniform Heat
Flow in a Sheet

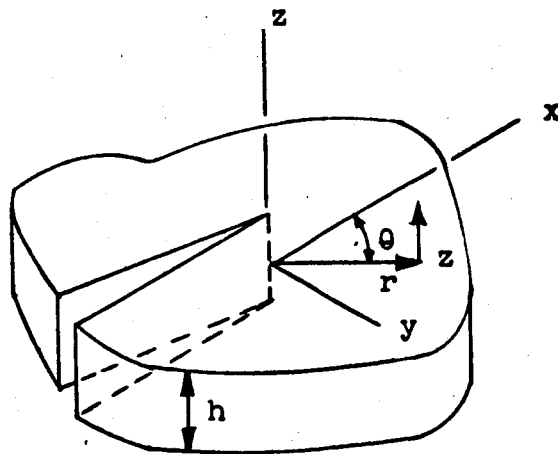


Figure 18 - Coordinates Used in a
Cracked Plate which will be
Subjected to Transverse Bending

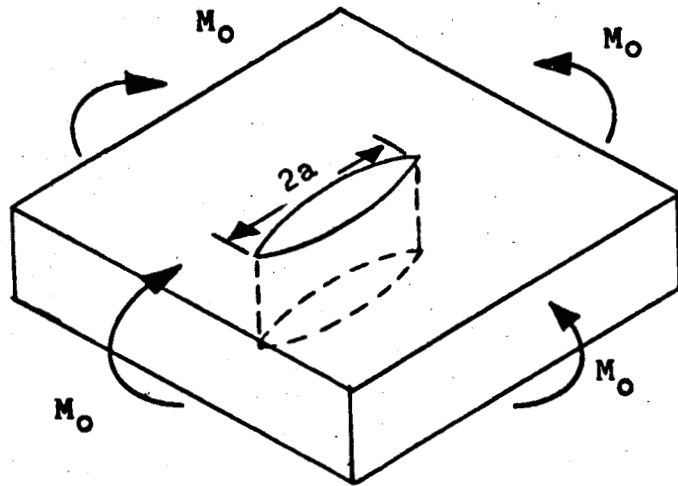


Figure 19 - A Through Crack in an
Infinite Plate Subjected to
Uniform Biaxial Bending

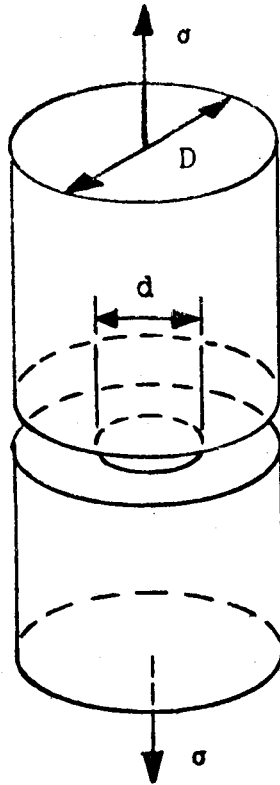


Figure 20 - A Circumferentially Cracked Round Bar Subjected to Tension

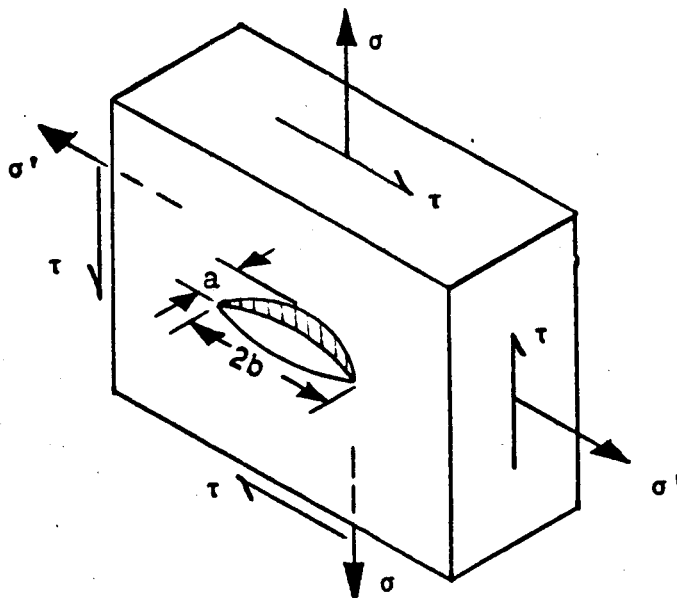


Figure 21 - A Semi-Elliptical Surface Crack in a Plate Subjected to General Extension

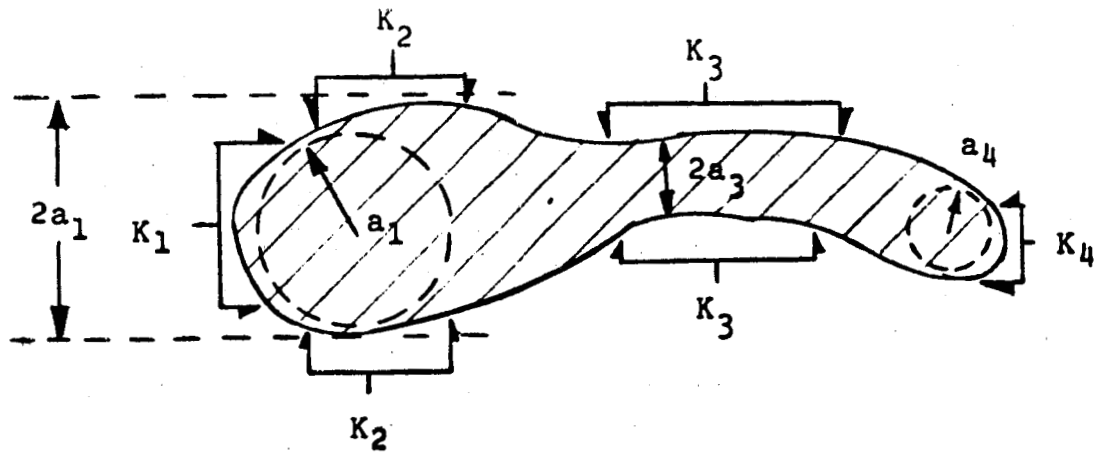


Figure 22 - The Plan View of an Irregular Crack in an Infinite Body

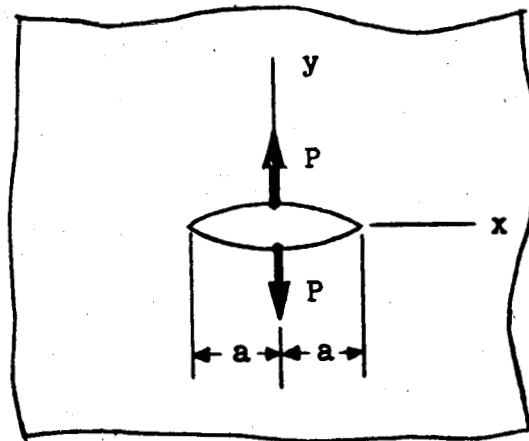


Figure 23 - A Crack in an Infinite Sheet Subjected to Centrally Applied Wedge Forces

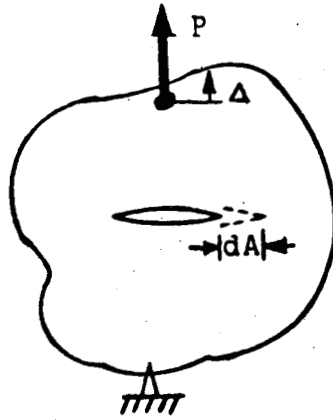


Figure 24 - A Crack in a Body of Arbitrary Shape Subjected to a Load

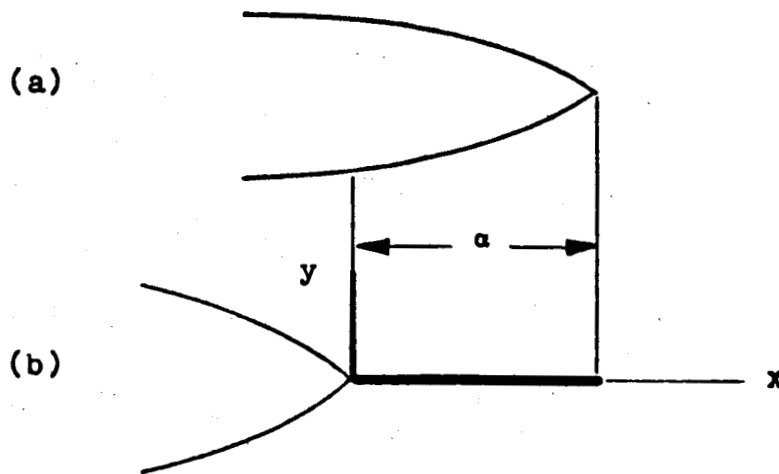


Figure 25 - The Tip of a Crack, (a), which has been pulled closed, (b), along a Segment Adjacent to the Tip

APPENDIX I - The Westergaard Method of Stress Analysis of Cracks

Any elementary text on the theory of elasticity gives a full development of the equations for plane extension. The equilibrium equations are:

$$\frac{\partial \sigma_x}{\partial x} + \frac{\partial \tau_{yx}}{\partial y} = 0$$
$$\frac{\partial \tau_{xy}}{\partial x} + \frac{\partial \sigma_y}{\partial y} = 0 \quad (114)$$

$$\tau_{xy} = \tau_{yx}$$

The strain-displacement relationships and Hooke's law lead to the comparability equation:

$$\nabla^2(\sigma_x + \sigma_y) = \left(\frac{\partial^2}{\partial x^2} + \frac{\partial^2}{\partial y^2} \right) (\sigma_x + \sigma_y) = 0 \quad (115)$$

The equilibrium equations (114) are automatically satisfied by defining an Airy's stress function, Φ , in terms of its relationship to the stresses, i.e.

$$\sigma_x = \frac{\partial^2 \Phi}{\partial y^2}$$
$$\sigma_y = \frac{\partial^2 \Phi}{\partial x^2}$$
$$\tau_{xy} = \frac{-\partial^2 \Phi}{\partial x \partial y} \quad (116)$$

Substituting equations (116) into (115) leads to:

$$\nabla^4 \bar{\phi} = \nabla^2(\nabla^2 \bar{\phi}) = 0 \quad (117)$$

In order to solve a problem the stress function, $\bar{\phi}$, must satisfy equation (117) and the boundary conditions of that problem.

Choosing the stress function, $\bar{\phi}$, to be:

$$\bar{\phi} = \psi_1 + x\psi_2 + y\psi_3 \quad (118)$$

it will automatically satisfy equation (117) if the ψ_i are each harmonic, i.e.

$$\nabla^2 \psi_i = 0 \quad (119)$$

Define a complex variable, z , by

$$z = x + iy \quad (120)$$

Functions of that complex variable, $\bar{Z}(z)$, and its derivatives,

$$\bar{Z} = \frac{d\bar{Z}}{dz}, \quad Z = \frac{dZ}{dz}, \quad Z' = \frac{dZ}{dz} \quad (121)$$

have harmonic real and imaginary parts, if the function is analytic, e.g. if: $\bar{Z} = \text{Re } \bar{Z} + i \text{Im } \bar{Z}$

$$\text{then: } \nabla^2(\text{Re } \bar{Z}) = \nabla^2(\text{Im } \bar{Z}) = 0 \quad (122)$$

This is a result of the Cauchy-Riemann conditions, i.e.

$$\frac{\partial \operatorname{Re} \bar{z}}{\partial x} = \frac{\partial \operatorname{Im} \bar{z}}{\partial y} = \operatorname{Re} z$$

$$\frac{\partial \operatorname{Im} \bar{z}}{\partial x} = -\frac{\partial \operatorname{Re} \bar{z}}{\partial y} = \operatorname{Im} z \quad (123)$$

equations (123) may be used to differentiate these functions \bar{z} through z .

First Mode

In conformity with equations (118) through (123) Westergaard [8] defined an Airy's stress function, ϕ , by

$$\phi_I = \operatorname{Re} Z_I + y \operatorname{Im} \bar{Z}_I \quad (124)$$

which as a consequence automatically satisfies equilibrium and compatibility, equations (114) and (117).

Using equations (116) and (123) the stresses resulting from ϕ , as defined in equation (124), are

$$\sigma_x = \operatorname{Re} Z_I - y \operatorname{Im} Z'_I$$

$$\sigma_y = \operatorname{Re} Z_I + y \operatorname{Im} Z'_I$$

$$\tau_{xy} = -y \operatorname{Re} Z'_I \quad (125)$$

Now any function, Z_I , which is analytic in the region except for a particular branch cut along a portion of the x-axis will have the form

$$Z_I = \frac{g(z)}{\sqrt{(z+b)(z-a)}} \quad (126)$$

This will solve crack problems for a crack along the x-axis from $x=-b$ to $x=a$, ($y=0$), if $g(z)$ is well behaved, since the stresses, σ_y and τ_{xy} , along that interval are zero, provided that

$$\text{Im } g(x) = 0 \quad (\text{for } -b < x < a) \quad (127)$$

For example if the function

$$Z_I = \frac{\sigma z}{\sqrt{z^2 - a^2}} \quad (128)$$

is examined, it solves the problem of a crack at $-a < x < a$, $y=0$ and leads to boundary conditions of uniform biaxial stress, σ , at infinity, see Figure 3.

Now, reverting to the more general case, equation (126), a substitution of variable

$$\zeta = z - a \quad (129)$$

leads to

$$Z_I = \frac{f(\zeta)}{\sqrt{\zeta}} \quad (130)$$

where from equation (126) and (127), $f(\mathfrak{z})$ is well behaved for small $|\mathfrak{z}|$, (i.e. near the crack tip at $x=a$). Moreover, in that region as $|\mathfrak{z}| \rightarrow 0$, g may be replaced by a real constant or equation (130) may be written

$$Z_I \Big|_{|\mathfrak{z}| \rightarrow 0} = \frac{K_I}{\sqrt{2\pi\mathfrak{z}}} \quad (131)$$

Other stress functions, Z_I , for crack problems, such as equation (16), will also always lead to this form.

Noting that equation (131) may be substituted into equations (125), and using polar coordinates, i.e.

$$\mathfrak{z} = r e^{i\theta} \quad (132)$$

the crack tip stress field is:

$$\begin{aligned} \sigma_x &= \frac{K_I}{\sqrt{2\pi r}} \cos \frac{\theta}{2} \left[1 - \sin \frac{\theta}{2} \sin \frac{3\theta}{2} \right] \\ \sigma_y &= \frac{K_I}{\sqrt{2\pi r}} \cos \frac{\theta}{2} \left[1 + \sin \frac{\theta}{2} \sin \frac{3\theta}{2} \right] \\ \tau_{xy} &= \frac{K_I}{\sqrt{2\pi r}} \sin \frac{\theta}{2} \cos \frac{\theta}{2} \cos \frac{3\theta}{2} \end{aligned} \quad (133)$$

where from equation (131)

$$K_I = \lim_{|\mathfrak{z}| \rightarrow 0} \sqrt{2\pi\mathfrak{z}} Z_I \quad (134)$$

The strain in the y-direction can be written in terms of displacements and stresses by Hooke's law, or

$$\epsilon_y = \frac{\partial v}{\partial y} = \frac{\sigma_y}{E} - \frac{\nu}{E} (\sigma_x + \sigma_z) \quad (135)$$

For plane strain Hooke's law ($\epsilon_z=0$) also leads to

$$\sigma_z = \nu(\sigma_x + \sigma_y) \quad (136)$$

Substituting equation (125) and (136) into equation (135) and integrating leads to

$$v = \frac{1+\nu}{E} [2(1-\nu) \operatorname{Im} Z_I - y \operatorname{Re} Z_I] \quad (137)$$

Similar consideration for ϵ_x gives

$$u = \frac{1+\nu}{E} [(1-2\nu) \operatorname{Re} Z_I - y \operatorname{Im} Z_I] \quad (138)$$

Substitution of equation (131) and (132) into equations (137) and (138) and noting $E = 2G(1+\nu)$ leads to

$$\begin{aligned} u &= \frac{K_I}{G} \sqrt{\frac{r}{2\pi}} \cos \frac{\theta}{2} [1-2 + \sin^2 \frac{\theta}{2}] \\ v &= \frac{K_I}{G} \sqrt{\frac{r}{2\pi}} \sin \frac{\theta}{2} [2-2 - \cos^2 \frac{\theta}{2}] \end{aligned} \quad (139)$$

(for plane strain, $w = 0$)

Equations (133), (134), (136) and (139) are the resulting crack tip stress and displacement fields, i.e. equations (1) and (13), for the first mode.

Second Mode

Instead of choosing the Airy's stress function as in equation (124), it is equally permissible to choose the form,

$$\Phi_{II} = -y \operatorname{Re} \bar{Z}_{II} \quad (140)$$

Repeating all of the operations from equation (124) through (139) and again making use of equations (114) through (123) leads to:

$$\begin{aligned} \sigma_x &= 2 \operatorname{Im} Z_{II} + y \operatorname{Re} Z'_{II} \\ \sigma_y &= -y \operatorname{Re} Z'_{II} \\ \tau_{xy} &= \operatorname{Re} Z_{II} - y \operatorname{Im} Z'_{II} \end{aligned} \quad (141)$$

and

$$\begin{aligned} u &= \frac{1+\nu}{E} [2(1-\nu) \operatorname{Im} \bar{Z}_{II} + y \operatorname{Re} Z_{II}] \\ v &= \frac{1+\nu}{E} [-(1-2\nu) \operatorname{Re} \bar{Z}_{II} - y \operatorname{Im} Z_{II}] \end{aligned} \quad (142)$$

and in the neighborhood of a crack tip, i.e. $|\mathcal{J}| \rightarrow 0$,

$$Z_{II} \Big|_{|\mathcal{J}| \rightarrow 0} = \frac{K_{II}}{\sqrt{2\pi\mathcal{J}}} \quad (143)$$

or

$$K_{III} = \lim_{|\mathcal{J}| \rightarrow 0} \sqrt{2\pi\mathcal{J}} Z_{III} \quad (144)$$

In addition, near the crack tip substitution of equation (143) into (141) and (142) leads to:

$$\begin{aligned} \sigma_x &= \frac{-K_{III}}{\sqrt{2\pi r}} \sin \frac{\theta}{2} \left[2 + \cos \frac{\theta}{2} \cos \frac{3\theta}{2} \right] \\ \sigma_y &= \frac{K_{III}}{\sqrt{2\pi r}} \cos \frac{\theta}{2} \left[1 - \sin \frac{\theta}{2} \cos \frac{3\theta}{2} \right] \\ \tau_{xy} &= \frac{K_{III}}{\sqrt{2\pi r}} \cos \frac{\theta}{2} \left[1 - \sin \frac{\theta}{2} \sin \frac{3\theta}{2} \right] \end{aligned} \quad (145)$$

and for plane strain

$$\begin{aligned} u &= \frac{K_{III}}{G} \sqrt{\frac{r'}{2\pi}} \sin \frac{\theta}{2} \left[2 - 2\nu + \cos^2 \frac{\theta}{2} \right] \\ v &= \frac{K_{III}}{G} \sqrt{\frac{r'}{2\pi}} \cos \frac{\theta}{2} \left[1 - 2\nu + \sin^2 \frac{\theta}{2} \right] \end{aligned} \quad (146)$$

These results are reflected in equations (2) and (14), for the second mode.

The first and second modes may be superimposed since

$$\Phi = \Phi_I + \Phi_{III} \quad (147)$$

is a perfectly permissible Airy's stress function in which case stress and displacement components should simply be added to each other.

Third Mode

The plane (2-dimensional) problem of pure shear may be specified by:

$$u = 0, v = 0, w = w(x,y) \quad (148)$$

The strain displacement equations and Hooke's law gives [111]:

$$\begin{aligned} \gamma_{xz} &= \frac{\partial w}{\partial x} = \frac{\tau_{xz}}{G} \\ \gamma_{yz} &= \frac{\partial w}{\partial y} = \frac{\tau_{yz}}{G} \end{aligned} \quad (149)$$

The stress components $\sigma_x, \sigma_y, \sigma_z$ and τ_{xy} all vanish so the equilibrium equations become

$$\frac{\partial \tau_{xz}}{\partial x} + \frac{\partial \tau_{yz}}{\partial y} = 0 \quad (150)$$

which when combined with equations (149) gives

$$\nabla^2 w = 0 \quad (151)$$

Choosing:

$$w = \frac{1}{G} \operatorname{Im} Z_{III} \quad (152)$$

leads to

$$\begin{aligned} \tau_{xz} &= \operatorname{Im} Z_{III} \\ \tau_{yz} &= \operatorname{Re} Z_{III} \end{aligned} \quad (153)$$

The stress function Z_{III} , for a crack along the negative y-axis to the origin, takes the form near the crack tip

$$Z_{III} \Big|_{|\mathcal{J}| \rightarrow 0} = \frac{K_{III}}{\sqrt{2\pi\mathcal{J}}} \quad (154)$$

Consequently,

$$K_{III} = \lim_{|\mathcal{J}| \rightarrow 0} \sqrt{2\pi\mathcal{J}} Z_{III} \quad (155)$$

Moreover, substituting equation (154) into equations (152) and (153) and using (132) leads to

$$\begin{aligned} \tau_{xz} &= -\frac{K_{III}}{\sqrt{2\pi r}} \sin \frac{\theta}{2} \\ \tau_{yz} &= \frac{K_{III}}{\sqrt{2\pi r}} \cos \frac{\theta}{2} \end{aligned} \quad (156)$$

and

$$w = \frac{K_{III}}{G} \sqrt{\frac{2r}{\pi}} \sin \frac{\theta}{2} \quad (157)$$

These results are reflected in equations (3) and (15) for the third mode.

APPENDIX II - A Handbook of Basic Solutions for Stress-
Intensity-Factors and other Formulas.

Appendix II will be supplied at a later date, only upon specific request, by clipping out this page, supplying name and address and mailing to:

Professor Paul C. Paris
Department of Mechanics
Lehigh University
Bethlehem, Pennsylvania

Name _____

Address _____

Appendix II - A Handbook of Basic Solutions for Stress-Intensity-Factors and Other Formulas

The results to be presented for stress-intensity-factors will conform with their definition as implied by equations (1), (2), (3), (48), (81) and (94). References which contain further results and details will be listed for the readers convenience.

A selection of solutions for stress-intensity-factors, in addition to those already listed, will be chosen on the basis of their generality. Since superposition may be used, i.e. addition of the stress-intensity-factors for each mode, the results which lend themselves to generation of other solutions will be emphasized.

- (1) Formulas for determination of stress-intensity-factors from stress concentrations [33].

Mode I:

$$K_I = \lim_{p \rightarrow 0} \frac{\sqrt{\pi}}{2} \sigma_{\max} \sqrt{p} \quad (158)$$

provided $K_{II}=K_{III}=0$ and where p is the tip radius of the notch and σ_{\max} is the maximum normal stress adjacent to the tip. (See equation (9))

Mode II:

$$K_{II} = \lim_{p \rightarrow 0} \sqrt{\pi} \sigma_{\max} \sqrt{p} \quad (159)$$

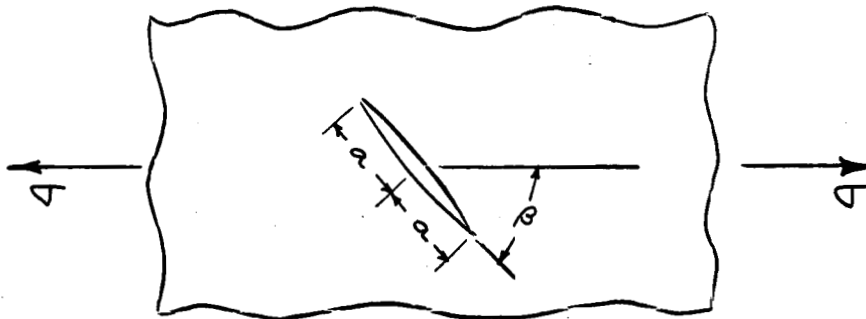
provided $K_I = K_{III} = 0$, etc.

Mode III:

$$K_{III} = \lim_{p \rightarrow 0} \sqrt{\pi} \tau_{\max} \sqrt{p} \quad (160)$$

provided $K_I = K_{II} = 0$ and where τ_{\max} is the maximum shear stress adjacent to the tip of the notch.

(2) Infinite sheets subjected to in plane loads.



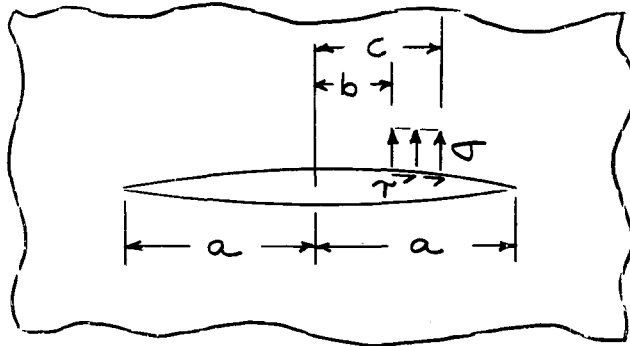
$$K_I = \sigma \sin^2 \beta \sqrt{\pi a} \quad (161)$$

$$K_{II} = \sigma \sin \beta \cos \beta \sqrt{\pi a}$$

$$\phi(\eta) = \frac{\sigma(1 - e^{2i\beta})a}{4\eta}$$

Ref.: [18] or via equations (33) or by superimposing results of equations (4) and (6). (Note that all other cases of uniform

loading at infinity or on the crack surface may be derived from this case by superposition.)



For the right end of the crack:

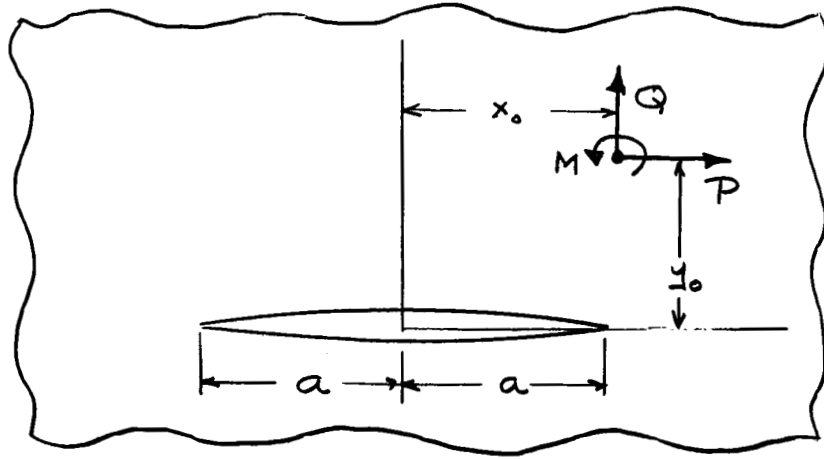
$$K_I = \frac{\sigma\sqrt{a}}{2\sqrt{\pi}} \left\{ \sin^{-1} \frac{c}{a} - \sin^{-1} \frac{b}{a} - \sqrt{1 - \frac{c^2}{a^2}} + \sqrt{1 - \frac{b^2}{a^2}} \right\} + \frac{\tau(c-b)}{2\sqrt{\pi a}} \left(\frac{\kappa-1}{\kappa+1} \right)$$

$$K_{II} = \frac{\sigma(c-b)}{2\sqrt{\pi a}} \left(\frac{\kappa-1}{\kappa+1} \right) + \frac{\tau\sqrt{a}}{2\sqrt{\pi}} \left\{ \sin^{-1} \frac{c}{a} - \sin^{-1} \frac{b}{a} - \sqrt{1 - \frac{c^2}{a^2}} + \sqrt{1 - \frac{b^2}{a^2}} \right\} \quad (162)$$

where $\kappa = 3-4\nu$ (plane stress)

or $\kappa = \frac{3-\nu}{1+\nu}$ (plane strain)

Ref.: Equations (32)

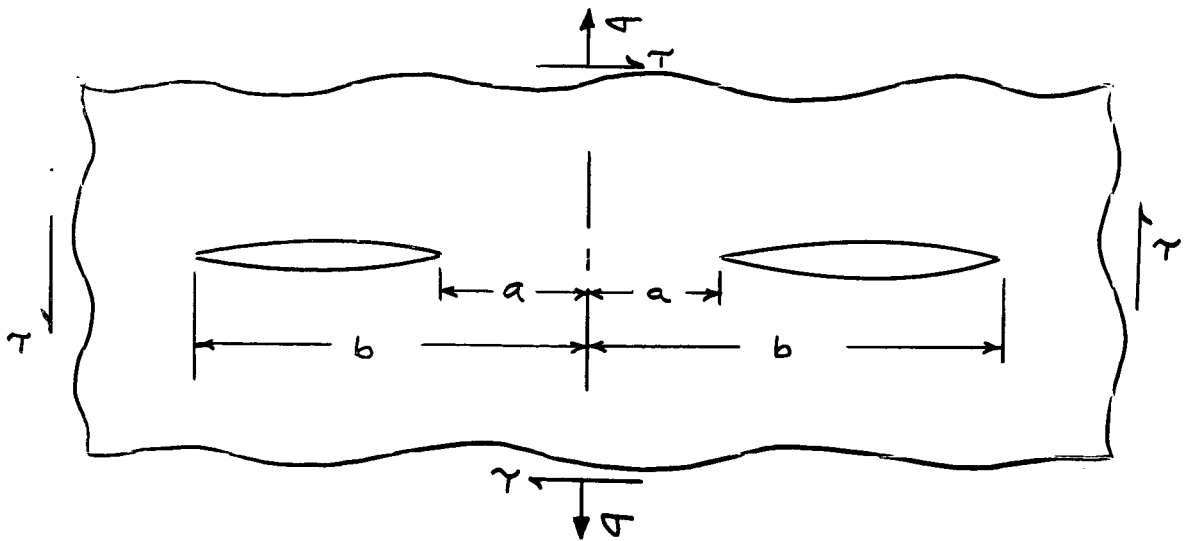


For the right end of the crack:

$$K = K_I - iK_{II} = \frac{1}{2\sqrt{\pi a}(1+k)} \left\{ (P+iQ) \left[\frac{a+z_0}{\sqrt{z_0^2-a^2}} - \frac{k(a+\bar{z}_0)}{\sqrt{\bar{z}_0^2-a^2}} - 1+k \right] + \frac{a(P-iQ)(\bar{z}_0-z_0) + ai(1+k)M}{(\bar{z}_0-a)\sqrt{\bar{z}_0^2-a^2}} \right\} \quad (163)$$

where: $z_0 = x_0 + iy_0$
 $\bar{z}_0 = x_0 - iy_0$

Ref. [21], [22] or via equations 33,
 (See also [23]).



At the near ends of two equal colinear cracks

$$K_I = \sigma \sqrt{\frac{\pi}{a}} \frac{b^2 \frac{E(k)}{K(k)} - a^2}{\sqrt{b^2 - a^2}}$$

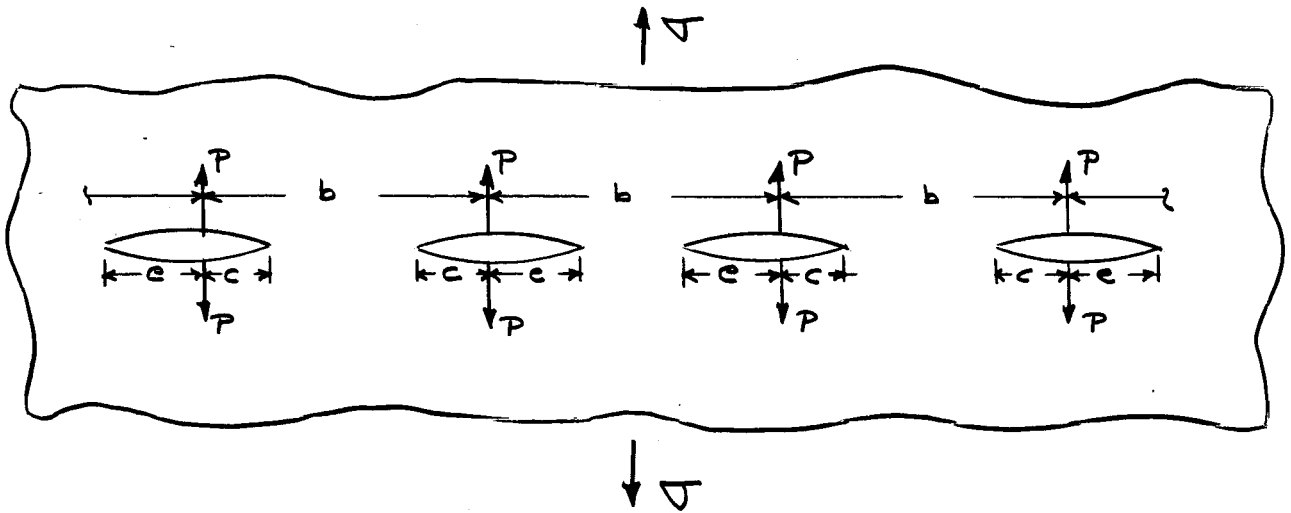
$$K_{II} = \tau \sqrt{\frac{\pi}{a}} \frac{b^2 \frac{E(k)}{K(k)} - a^2}{\sqrt{b^2 - a^2}} \quad (164)$$

At the far ends:

$$K_I = \sigma \sqrt{\pi b} \left(\frac{1}{k} - \frac{E(k)}{kK(k)} \right)$$

$$K_{II} = \tau \sqrt{\pi b} \left(\frac{1}{k} - \frac{E(k)}{kK(k)} \right) \quad (165)$$

where $k = \sqrt{1 - \frac{a^2}{b^2}}$ is the modulus of the complete elliptic integrals $E(k)$ and $K(k)$ of the first and second kind, respectively. Ref. [38], [23], (See also [21] for concentrated forces on the crack surface.)

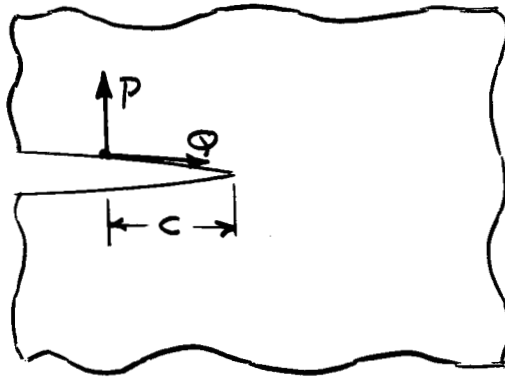


For an infinite array of cracks at the ends denoted by e :

$$K_I = \frac{\sigma \sqrt{4b} \sin \frac{\pi e}{2b}}{\sqrt{\cos \frac{\pi e}{2b} \left(\sin \frac{\pi e}{2b} + \sin \frac{\pi c}{2b} \right)}} + \frac{P \sqrt{\sin \frac{\pi c}{2b}}}{\sqrt{b \sin \frac{\pi e}{2b} \cos \frac{\pi e}{2b} \left(\sin \frac{\pi e}{2b} + \sin \frac{\pi c}{2b} \right)}}$$

$$K_{II} = 0 \quad (166)$$

Ref.: G.R. Irwin (unpublished N.R.L. Report), (See also [4] and [5].) (Note that this result may be used to evaluate eccentrically located cracks in pannels.)

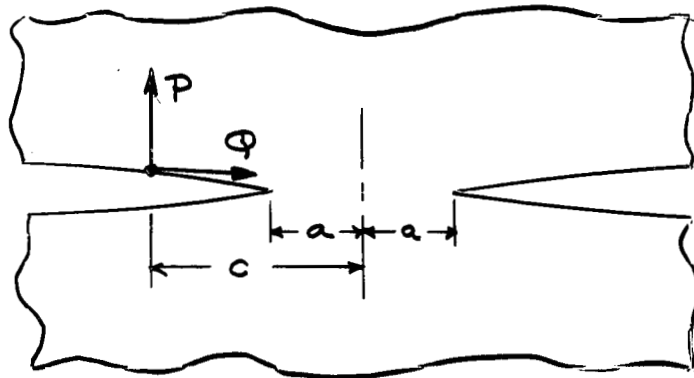


For a semi-infinite crack:

$$K_I = \frac{P}{\sqrt{2\pi c}}$$

$$K_{II} = \frac{Q}{\sqrt{2\pi c}} \quad (167)$$

Ref.: Equations (32) or [21]



For two semi-infinite cracks;

At the left crack tip:

$$K_I = \frac{P \sqrt{c^2 - a^2}}{2\sqrt{\pi a} (c - a)}$$

$$K_{II} = \frac{Q \sqrt{c^2 - a^2}}{2\sqrt{\pi a} (c-a)}$$

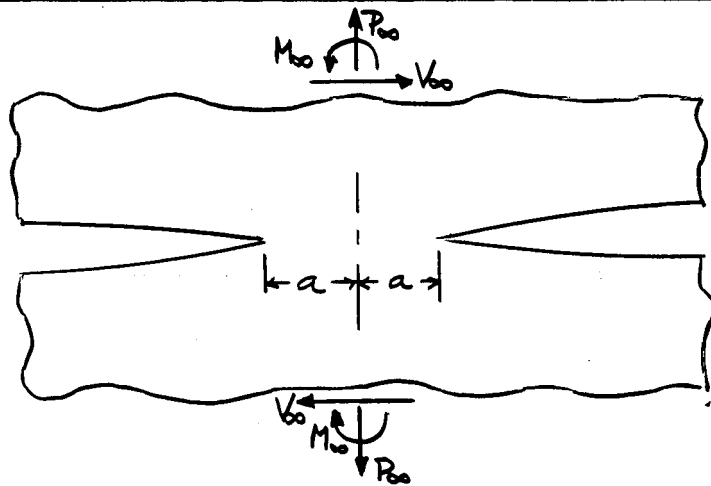
At the right crack tip:

$$K_I = \frac{P \sqrt{c^2 - a^2}}{2\sqrt{\pi a} (c+a)}$$

$$K_{II} = \frac{Q \sqrt{c^2 - a^2}}{2\sqrt{\pi a} (c+a)}$$

(168)

Ref.: [21]



Stress concentrations for deep hyperbolic notches are [10];
for P_∞ (force per unit thickness) alone:

$$\frac{\sigma_{\max}}{\sigma_{\text{net}}} = \frac{2 \sqrt{\frac{a}{p}} (1 + \frac{p}{a})}{(1 + p/a) \tan^{-1} \sqrt{\frac{a}{p}} + \sqrt{\frac{p}{a}}}$$

$$\sigma_{\text{net}} = \frac{P_\infty}{2a}$$

(169)

For V_∞ alone:

$$\frac{\sigma_{\max}}{\tau_{\text{net}}} = \frac{\sqrt{\frac{a}{p} + 1}}{(1 + \frac{p}{a}) \tan^{-1} \sqrt{\frac{a}{p}} - \sqrt{\frac{p}{a}}}$$
$$\tau_{\text{net}} = \frac{V_\infty}{2a} \quad (170)$$

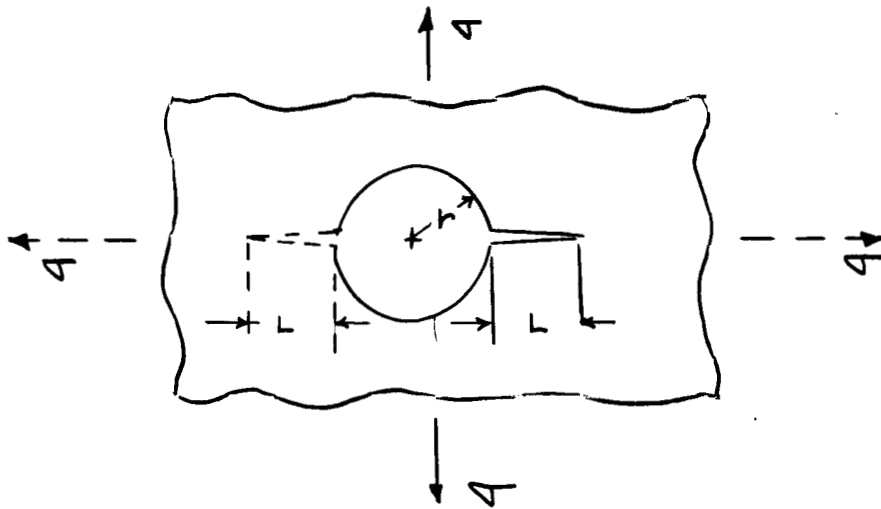
For M_∞ alone:

$$\frac{\sigma_{\max}}{\sigma_{\text{net}}} = \frac{4 \sqrt{\frac{a}{p}}}{3 \left[\sqrt{\frac{p}{a}} + (1 - \frac{p}{a}) \tan^{-1} \sqrt{\frac{a}{p}} \right]}$$
$$\sigma_{\text{net}} = \frac{3 M_\infty}{2 a^2} \quad (171)$$

Using equations (158) and (159), for the right crack tip:

$$K_I = \frac{P_\infty}{\sqrt{\pi a}} + \frac{2 M_\infty}{\sqrt{\pi} a^{3/2}}$$
$$K_{II} = \frac{V_\infty}{\sqrt{\pi a}} \quad (172)$$

Ref. [10], [33], [45]



For Cracks Emanating from a Circular Hole

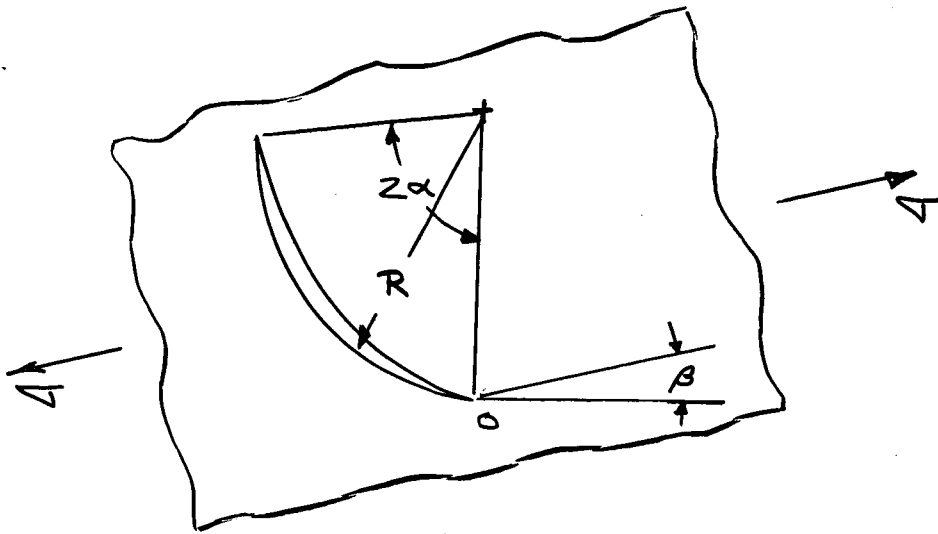
$$K_I = \sigma \sqrt{L\pi} \quad F\left(\frac{L}{r}\right)$$

$$K_{II} = 0$$

(173)

$\frac{L}{r}$	One Crack		Two Cracks	
	$F\left(\frac{L}{r}\right)$ (uniaxial stress)	$F\left(\frac{L}{r}\right)$ (biaxial stress)	$F\left(\frac{L}{r}\right)$ (uniaxial stress)	$F\left(\frac{L}{r}\right)$ (biaxial stress)
0.00	3.39	2.26	3.39	2.26
0.10	2.73	1.98	2.73	1.98
0.20	2.30	1.82	2.41	1.83
0.30	2.04	1.67	2.15	1.70
0.40	1.86	1.58	1.96	1.61
0.50	1.73	1.49	1.83	1.57
0.60	1.64	1.42	1.71	1.52
0.80	1.47	1.32	1.58	1.43
1.0	1.37	1.22	1.45	1.38
1.5	1.18	1.06	1.29	1.26
2.0	1.06	1.01	1.21	1.20
3.0	0.94	0.93	1.14	1.13
5.0	0.81	0.81	1.07	1.06
10.0	0.75	0.75	1.03	1.03
∞	0.707	0.707	1.00	1.00

Ref.: [40]

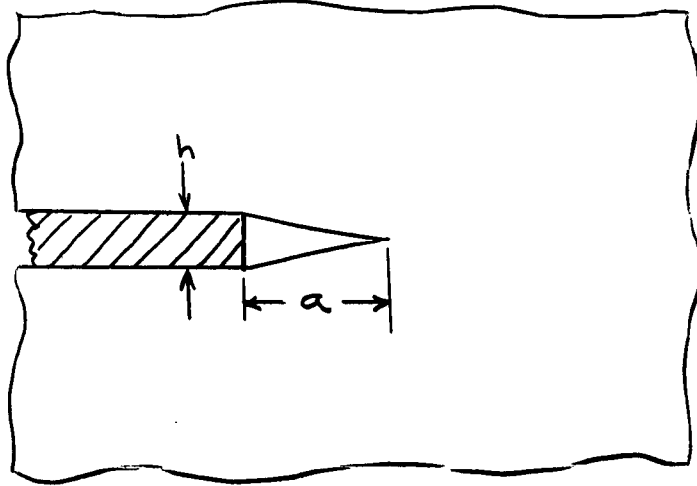


For the crack tip at o:

$$\begin{aligned}
 K_{\text{I}} &= \frac{\sigma(\pi R \sin \alpha)^{1/2}}{2(1 + \sin^2 \frac{\alpha}{2})} \left\{ \begin{aligned} &\cos \frac{\alpha}{2} + \cos (2\beta + \frac{5}{2}\alpha) [\sin^2 \frac{\alpha}{2}] \\ &- \cos (2\beta + \frac{3}{2}\alpha) [\cos^2 \frac{\alpha}{2} - \sin^4 \frac{\alpha}{2}] \\ &- \sin (2\beta + \frac{3}{2}\alpha) [\sin \alpha \sin^2 \frac{\alpha}{2}] \end{aligned} \right\} \\
 K_{\text{II}} &= \frac{\sigma(\pi R \sin \alpha)^{1/2}}{2(1 + \sin^2 \frac{\alpha}{2})} \left\{ \begin{aligned} &\sin \frac{\alpha}{2} + \sin (2\beta + \frac{5}{2}\alpha) [\sin^2 \frac{\alpha}{2}] \\ &+ \sin (2\beta + \frac{3}{2}\alpha) [\cos^2 \frac{\alpha}{2} - \sin^4 \frac{\alpha}{2}] \\ &- \cos (2\beta + \frac{3}{2}\alpha) [\sin \alpha \sin^2 \frac{\alpha}{2}] \end{aligned} \right\} \quad (174)
 \end{aligned}$$

Ref.: [18]

(3) Some cases of specified displacements in infinite planes

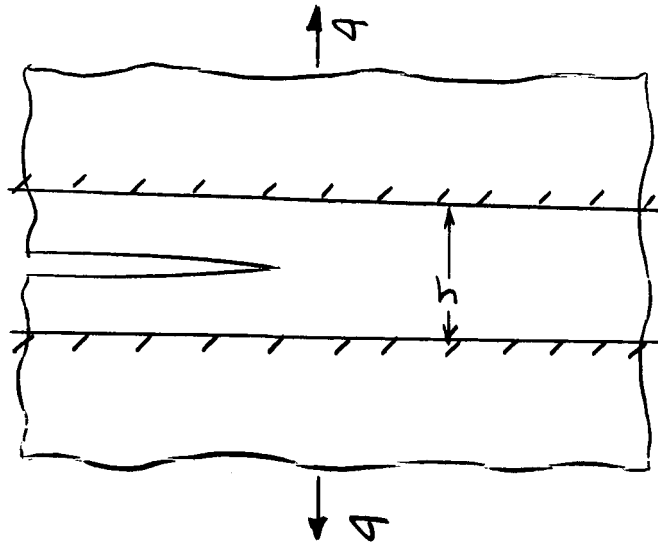


For an infinite rigid wedge of constant thickness:

$$K_I = \frac{Eh}{\sqrt{2\pi a}} \quad (\text{for plane stress})$$

$$K_{II} = 0 \quad (177)$$

Ref.: [23] (Also see [23] for discussion of other examples of wedging)



The following sequence of events:

- 1) Stress applied
- 2) Boundaries clamped
- 3) Crack introduced

Results in constant energy release rate, G_I , or

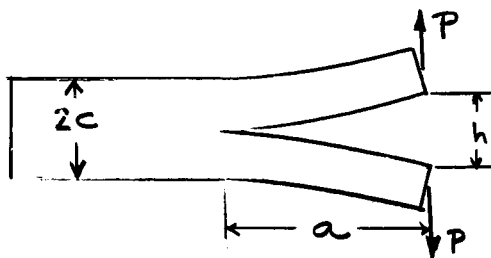
$$K_I = \frac{\sigma \sqrt{h}}{\sqrt{2}}$$

$$K_{II} = 0$$

(178)

Ref.: [45]

(4) A case of the splitting of rods



A slender rectangular member ($a \gg 2c$),

Under wedging:

$$K_I = \frac{\sqrt{3} E h c^{3/2}}{4 a^2} \quad (179)$$

$$K_{II} = 0$$

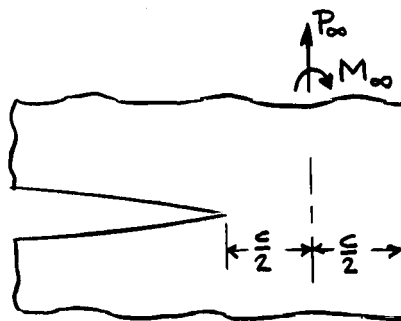
or under forces:

$$K_I = \frac{2 \sqrt{3} P a}{c^{3/2}}$$

$$K_{II} = 0 \quad (180)$$

Ref.: [23] (or see J.J. Gilman, Fracture (ed. by Averbach et.al.)
John Wiley & Sons, New York, 1959)

(5) A semi-infinite notch approaching the free edge of a
half-plane

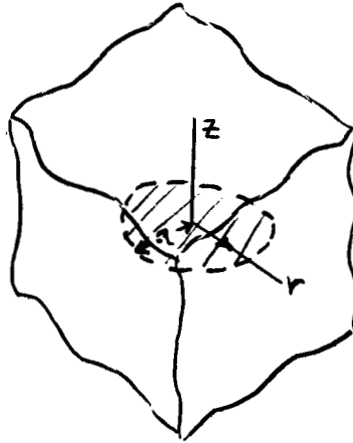


$$K_I = \sqrt{\pi} \left(\frac{4\pi - 12}{\pi^2 - 8} \right) \frac{P_\infty}{\sqrt{c}} + \sqrt{\pi} \left(\frac{4\pi - 8}{\pi^2 - 8} \right) \frac{M_\infty}{c^{3/2}} \quad (181)$$

$$K_{II} = 0$$

Ref.: [10], [39]

(6) Axisymmetrical loading of a body with a circular disk crack

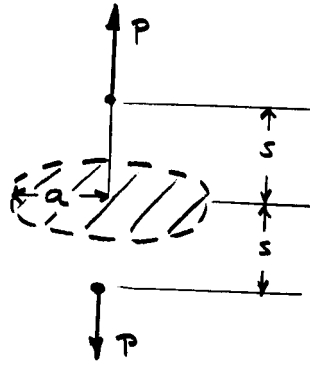


For an axisymmetrical normal pressure distribution, $p(r)$,
on both crack surfaces

$$K_I = \frac{2}{\sqrt{\pi a}} \int_0^a \frac{r p(r)}{\sqrt{a^2 - r^2}} dr$$

$$K_{II} = 0 \quad (182)$$

Ref.: [23] (Note that with superposition this enables treatment
of all cases of axisymmetrical loading)

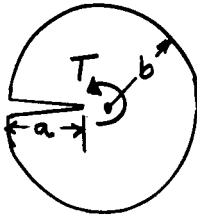


$$K_I = \frac{P}{(\pi a)^{3/2}} \frac{[1 + (\frac{2-\nu}{1-\nu}) \frac{s^2}{a^2}]}{[1 + \frac{s^2}{a^2}]^2}$$

$$K_{II} = 0 \quad (183)$$

Ref.: [23] or using equations (182)

(7) Torsion and beam shear of prismatical bars with cracks



$$K_I = K_{II} = 0$$

$$K_{III} = \frac{(1+\alpha)^{3/2} (1-\alpha)^3 [2(1-\alpha) + \sqrt{\alpha}(mJ_0 + J_1)] \sqrt{\pi} T}{\alpha^2 \{2\pi^2 - [2(1-\alpha)^2 A^2 + \alpha(A+B)^2]\} a^{5/2}} \quad (184)$$

where

$$\alpha = \frac{b-a}{b}$$

$$m = 1/2 \left(\alpha + \frac{1}{\alpha} \right)$$

$$J_0 = 4 \arctan \sqrt{\alpha}$$

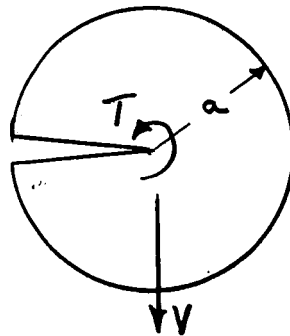
$$J_1 = \frac{-(1-\alpha)}{4\alpha} [4\sqrt{\alpha} - (1-\alpha)J_0]$$

$$A = 1/\alpha \left[(1+\alpha)^2 \frac{\arctan \sqrt{\alpha}}{\sqrt{\alpha}} - (1-\alpha) \right]$$

and

$$B = \frac{1-\alpha}{\alpha} [2 - 3/4(1-\alpha)A]$$

Ref.: [26] (Note that several other configurations are treated in [24], [25], and [26]).

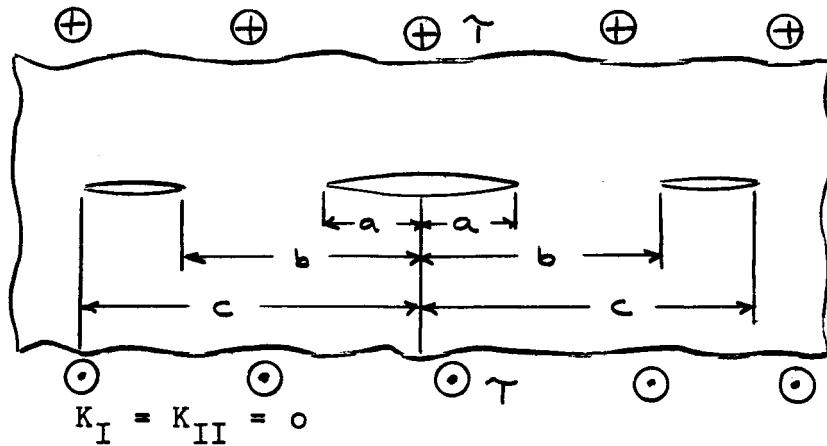


$$K_I = K_{II} = 0$$

$$K_{III} = 0.969 \frac{T}{a^{5/2}} - \left(\frac{6.95 + 6.47\nu}{1+\nu} \right) \frac{V}{a^{3/2}} \quad (185)$$

Ref.: [26], [24]

(8) Cracks under longitudinal (pure) shear



For the crack tips at a:

$$K_{III} = \pm \sqrt{\frac{c^2 - a^2}{b^2 - a^2}} \frac{E(k)}{K(k)} \tau \sqrt{\pi a}$$

For the crack tips at b:

$$K_{III} = \pm \sqrt{\frac{b^2 - a^2}{c^2 - b^2}} \left[1 - \left(\frac{c^2 - a^2}{b^2 - a^2} \right) \frac{E(k)}{K(k)} \right] \tau \sqrt{\pi b}$$

For the crack tips at c:

$$K_{III} = \pm \sqrt{\frac{c^2 - a^2}{c^2 - b^2}} \left[1 - \frac{E(k)}{K(k)} \right] \tau \sqrt{\pi c}$$

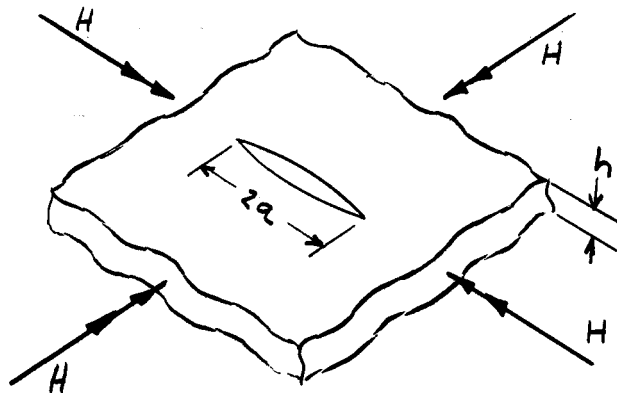
where

$$k = \sqrt{\frac{c^2 - a^2}{c^2 - b^2}}$$

is the modulus of the complete elliptic integrals, $E(k)$ and $K(k)$ of the first and second kind, respectively.

Ref.: G.C. Sih "Boundary Problems for Longitudinal Shear Cracks"
 Proc. of 2nd Conf. on Theor. and Appl. Mech., Pergamon Press, 1964.

(9) The flexure of infinite plates



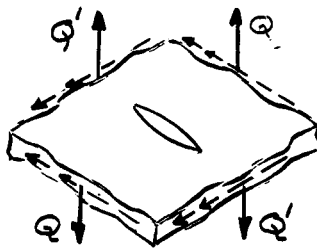
A plate subjected to pure twisting moment (per unit length), H , at infinity gives:

$$\phi(\eta) = - \frac{iHa}{2D(3+\nu)\eta}$$

or

$$\begin{aligned} K_B &= 0 \\ K_S &= \frac{6H}{h^2} \sqrt{\pi a} \end{aligned} \quad (187)$$

Ref.: [18], [33]



Uniform shear (per unit length), Q , at infinity (moments required for equilibrium shown dotted) gives:

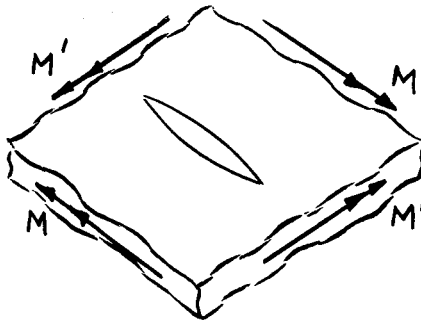
$$\psi(\eta) = \frac{Q a^2}{12 D} \left[\eta^2 + \left(\frac{1-\nu}{3+\nu} \right) \frac{3}{\eta^2} \right]$$

or

$$\begin{aligned} K_B &= 0 \\ K_S &= \frac{8\sqrt{\pi}Q a^{3/2}}{h^2} \end{aligned} \quad (188)$$

(Results independent of Q')

Ref.: [18]

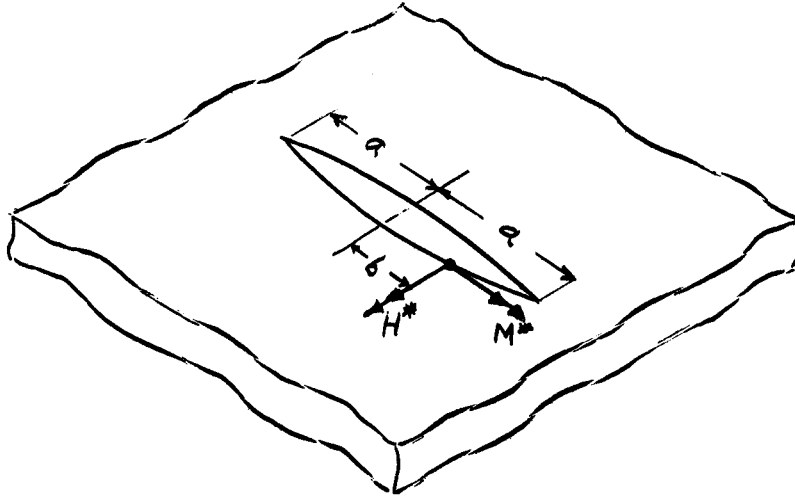


For uniform moments at infinity

$$\begin{aligned} K_B &= \frac{6M}{h^2} \sqrt{\pi a} \\ K_S &= 0 \end{aligned} \quad (189)$$

(Results independent of M')

Ref.: [18]



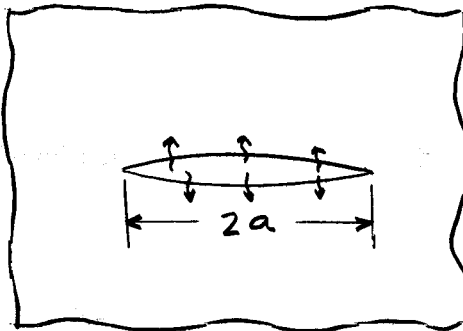
For a concentrated couple on the crack surface

$$K_B = \frac{3M^*}{h^2 \sqrt{\pi a}} \sqrt{\frac{a+b}{a-b}} + \frac{3H^*}{2h^2 \sqrt{\pi a}} (1+\nu)$$

$$K_S = \frac{3M^*}{2h^2 \sqrt{\pi a}} (1+\nu) - \frac{3H^*}{h^2 \sqrt{\pi a}} \sqrt{\frac{a+b}{a-b}} \quad (190)$$

Ref.: [33]

(10) Thermal stress problems



A plate with uniform temperature supplied on the crack surface gives

$$K_I = - \frac{E \alpha \sqrt{a} \dot{q}}{\sqrt{\pi} (1+k) \mu}$$

$$K_{II} = 0 \quad (191)$$

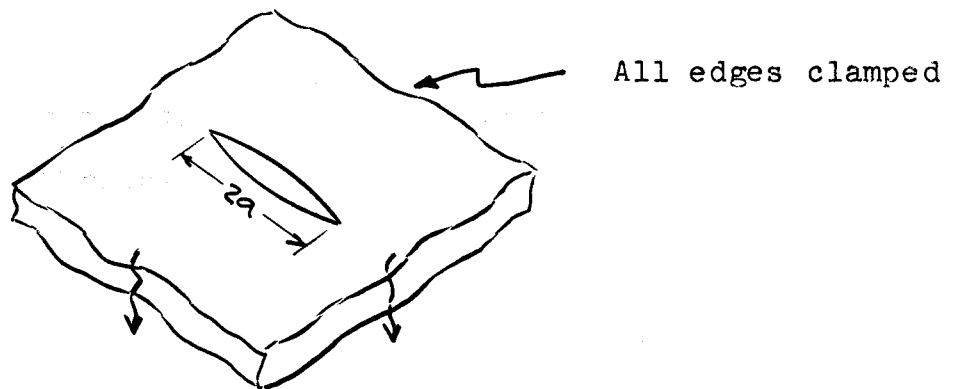
where

μ = thermal conductivity

\dot{q} = rate of total heat
per unit thickness supplied
to the plate

Ref.: [51]

(Note that this case has significance for high pressure
gas escaping through a crack)

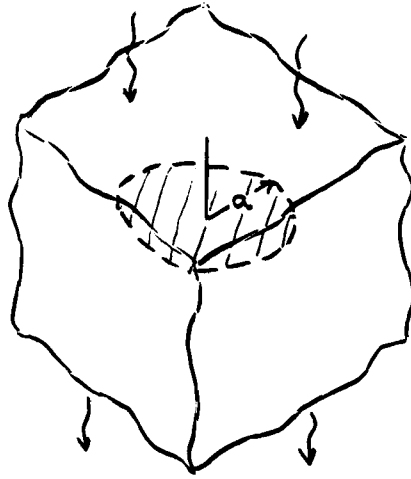


A clamped plate with a thermal gradient through the thickness
gives:

$$K_B = \frac{\alpha E h \Delta T \sqrt{\pi a}}{2(1-\nu)}$$

$$K_S = 0 \quad (192)$$

Ref.: [51]



An infinite body with an circular disk crack perpendicular to a thermal gradient gives:

$$K_{II} = \frac{E\alpha \Delta T a^{3/2}}{3 \pi (1-\nu)}$$

$$K_I = K_{III} = 0 \quad (193)$$

Ref.: A.L. Florence and J.N. Goodier "The Linear Thermoelastic Problem of Head Flow Disturbed by a Pennyshaped Insulated Crack" Internat. Journ. of Engin. Sc., Vol. 1, No.4, Dec. 1963.